

Doctoral Dissertation (Censored)

博士論文（要約）

A study on CLE peptides as abiotic and biotic mediators

(非生物的及び生物的环境応答因子としてのCLEペプチドの研究)

A Dissertation Submitted for the Degree of Doctor of Philosophy

July 2020

令和 2 年 7 月博士（理学）申請

Department of Biological Sciences, Graduate School of Science

The University of Tokyo

東京大学大学院理学系研究科

生物科学専攻

Ma Dichao

馬 笛超

Contents

	Acknowledgements	1
	List of Abbreviations	2
	Abstract	4
Chapter I	Introduction	6
Chapter II	Materials and Methods	10
Chapter III	Results	15
III-1	Expression of <i>CLE1–CLE7</i> in response to abiotic stimuli	
III-2	Function of <i>CLE2</i> and <i>CLE3</i> in the dark	
III-3	Downstream components of the CLE2 signaling pathway	
Chapter IV	Discussion	21
IV-1	Expression profiles of <i>CLE1–CLE7</i> in response to different environmental stimuli	
IV-2	Functions of CLE2 peptide	
IV-3	Functions of CLE3 peptide	
IV-4	Roles of <i>CLE2</i> and <i>CLE3</i> as mediators of environmental stimuli	
	Tables and Figures	25
	References	60

Acknowledgements

I want to express my deepest appreciation to Prof. Hiroo Fukuda and Prof. Kyoko Ohashi-Ito for giving me this opportunity to study in this laboratory. Their supervision and encouragement guided me time after time throughout this study. I sincerely appreciate Prof. Mitsutomo Abe, Prof. Ichiro Terashima, Prof. Munetaka Sugiyama and Prof. Tetsuya Higashiyama for their reviews and comments on this dissertation. I also want to express my sincere gratitude to Dr. Satoshi Endo, who helped me uncountable times in my study and research processes. I would like to offer my special thanks to Dr. Shigeyuki Betsuyaku for experimental support and valuable advice. I also thank Dr. Kuninori Iwamoto, Miss. Yasuko Ozawa, Miss. Yukiko Sugisawa and Mr. Masakazu Ota for technical support. I appreciate Dr. Xiaofeng Yin for his patient grammar check. Finally, I thank all other lab members for their encouragement.

List of abbreviations

35S	35S promoter of cauliflower mosaic virus
ABA	Absciscic acid
ACR4	ARABIDOPSIS CRINKLY 4
BAM	BARLEY NO MERISTEM
BSK1	BRASSINOSTEROID-SIGNALING KINASE 1
Cas9	CRISPR-associated 9
cDNA	Complementary DNA
CLE	CLAVATA3/EMBRYO SURROUNDING REGION-RELATED
CLE-RS2	CLAVATA3/ESR (CLE)-RELATED-ROOT SIGNAL 2
CLV3	CLAVATA3
CRISPR	Clustered regularly interspaced short palindromic repeats
CRN	CORYNE
DEFL	Defensin-like
DIN10	DARK INDUCIBLE 10
DMSO	Dimethyl sulfoxide
ERF	ETHYLENE RESPONSE FACTOR
EXT	EXTENSIN
GO	Gene ontology
GUS	β -glucuronidase
HAR1	HYPERNODULATION ABERRANT ROOT FORMATION 1
HSL1	HAESA-LIKE 1
LRR-RLK	Leucine-rich repeat receptor-like kinase

LLP1	LIGAND LIKE PROTEIN 1
MS	Murashige and Skoog
N	Nitrogen
PXY	PHLOEM INTERCALATED WITH XYLEM
qRT-PCR	Quantitative reverse transcription PCR
RAM	Root apical meristem
RLK7	RECEPTOR-LIKE KINASE 7
RPK2	RECEPTOR-LIKE PROTEIN KINASE 2
SAM	Shoot apical meristem
SAUR	SMALL AUXIN UP RNA
SOL2	SUPPRESSOR OF LLP1 2
T6P	Trehalose-6-phosphate
TDIF	Tracheary element differentiation inhibitory factor
TDR	TDIF receptor
TOAD2	TOADSTOOL 2
WOX4	WUSCHEL-RELATED HOMEODOMAIN 4
WT	Wild-type
WUS	WUSCHEL

Abstract

Plants sense environmental stimuli and convert them into cellular signals, which are transmitted to distinct cells and tissues to induce adequate responses. Plant hormones and small secretory peptides such as CLAVATA3/EMBRYO SURROUNDING REGION-RELATED (CLE) peptides often function as environmental stress mediators. In this study, I investigated whether and how CLE1–CLE7 peptides, which share the CLE domain with high sequence similarity, mediate environmental stimuli in *Arabidopsis thaliana*.

I investigated the expression of *CLE1–CLE7* genes upon various abiotic stimuli. *CLE1–CLE7* responded to different environmental stimuli, such as nitrogen deprivation, nitrogen replenishment, cold, salt and dark in a sophisticated manner (Chapter III-1). In addition, I found that dark treatment could induce *CLE2* and *CLE3* expression in roots (Chapter III-2). To further investigate *CLE2* and *CLE3* functions, I generated knockout mutants and estradiol inducible overexpressors. The phenotypic analysis revealed that *cle2* showed a chlorosis phenotype under light-deficient condition (Chapter III-2). This result suggests that *CLE2* was required for light-deficient responses. Using the estradiol inducible *CLE2* overexpressor, I found that induction of *CLE2* in roots induced the expression of various genes not only in roots but also in shoots, and genes related to light-dependent carbohydrate metabolism were particularly induced in shoots (Chapter III-3). These results together suggest that root-induced *CLE2* functions systemically in light-dependent carbohydrate metabolism in shoots.

In conclusion, I found that *CLE2* and *CLE3* peptides, CLE domains of which differ by only a single amino acid, play distinctive roles in shade response. This finding provide a concept that, in

addition to their functional redundancy, similar CLE1–CLE7 peptides may be involved in distinctive environmental responses to maintain the robust adaptive capacity in *Arabidopsis* plants.

Chapter I: Introduction

Plants have to withstand severe environmental fluctuations. To adapt to various environments, plants have evolved excellent sensing and response systems. Plants perceive environmental cues with a high sensitivity, convert these cues into cellular signals, transduce these signals to distinct cells and tissues, and induce adequate responses. Plants produce various signaling molecules that mediate environmental stimuli to specific cellular responses. Plant hormones are well-known mediators of environmental stresses (Verma et al. 2016). For example, the plant hormone abscisic acid (ABA) acts as a mediator of dehydration (Bray 1997; Bonetta and McCourt 1998; Shinozaki and Yamaguchi-Shinozaki 1997; Shinozaki and Yamaguchi-Shinozaki 2000; Finkelstein et al. 2002; Sato et al. 2018). Recent reports indicate that small secretory peptides, such as CLAVATA3/EMBRYO SURROUNDING REGION-RELATED (CLE), also function as mediators of environmental stimuli (Okamoto et al. 2009; Suzuki et al. 2011; Araya et al. 2014; Takahashi et al. 2018; Zhang et al. 2019).

The *Arabidopsis thaliana* genome contains 32 *CLE* genes, each of which encodes a preproprotein containing a secretion signal peptide at the N-terminus and a conserved 12 or 13-amino-acid CLE domain at the C-terminus (Oelkers et al. 2008; Ohyama et al. 2009). The CLE domain is a crucial functional region (Ito et al. 2006), which undergoes processing to form the mature CLE peptide (Matsubayashi 2011). After being secreted to extracellular matrix, these signaling peptides are perceived by corresponding plasma membrane-localized leucine-rich repeat receptor-like kinases (LRR-RLKs), thereby activating specific downstream signaling pathways in the cells. In the CLE family, *CLAVATA3* (*CLV3*) and *CLE40* are responsible for the maintenance of the shoot apical meristem (SAM) and the root apical meristem (RAM) by regulating the expression of the

homeodomain transcription factors, *WUSCHEL* (*WUS*) and *WUSCHEL-RELATED HOMEODOMAIN 5* (*WOX5*), respectively (Mayer et al. 1998; Brand et al. 2000; Schoof et al. 2000; Hobe et al. 2003; Stahl et al. 2009). Three major receptor complexes of CLV1, CLV2-SUPPRESSOR OF *CLV1* 2 (*SOL2*)/CORYNE (CRN), and RECEPTOR-LIKE PROTEIN KINASE 2 (*RPK2*)/TOADSTOOL 2 (*TOAD2*) are required to transmit the CLV3 signal in the SAM (Clark et al. 1996; Kayes and Clark 1998; Sawa 2006; Han et al. 2020), whereas CLE40 is recognized by the receptor kinase ARABIDOPSIS CRINKLY 4 (*ACR4*), thereby regulating *WOX5* expression in the RAM (Stahl et al. 2009). In the vascular meristem, *CLE41* and *CLE44* encode TRACHEARY ELEMENT DIFFERENTIATION INHIBITORY FACTOR (TDIF) regulating *WUSCHEL-RELATED HOMEODOMAIN 4* (*WOX4*) expression, which contributes to the balanced maintenance of vascular stem cells. TDIF RECEPTOR/PHLOEM INTERCALATED WITH XYLEM (*TDR/PXY*) perceives the TDIF ligand that is secreted from phloem to regulate *WOX4* expression in procambium (Ito et al. 2006; Hirakawa et al. 2008; Hirakawa et al. 2010; Zhang et al. 2016; Morita et al. 2016). In addition, a recent study also showed that CLE9 and CLE10 peptide regulates two different process, stomatal lineage and xylem development, through HAESA-LIKE 1 (*HSL1*) and BARLEY NO MERISTEM (*BAM*) receptor kinases, respectively (Qian et al. 2018).

Mature CLE1–CLE7 peptides have close phylogenetic relationship (Kucukoglu and Nilsson 2015) and similar or identical amino acid sequences (Fig. 1; Ito et al. 2006). In contrast to most of CLE peptides, application of synthetic CLE1–CLE7 peptides to plants did not cause visible phenotype such as root growth defect or abnormal vascular development (Kinoshita et al. 2007; Kondo et al. 2011). Expression of *CLE1* or *CLE6* under the control of the *CLV3* promoter almost fully complements the enlarged shoot apical meristem phenotype of *clv3* mutants, most likely through the *CLV1*-dependent pathway (Ni and Clark 2006). Transgenic lines overexpressing *CLE2*–

CLE7 genes under the control of *Cauliflower Mosaic Virus 35S* promoter exhibit similar late flowering and semi-dwarf phenotypes (Strabala et al. 2006). Overexpression of *CLE6* also partly compensates the shoot dwarfism phenotype associated with gibberellic acid (GA) deficiency (Bidadi et al. 2014). A recent study suggests that *CLE5* and *CLE6* function downstream of the leaf patterning factors and phytohormones to modulate the final leaf morphology (DiGennaro et al. 2018). However, *cle1* and *cle7* loss-of-function mutant lines as well as the *cle3* knockdown mutant line show no detectable morphological defects in development of seedlings, inflorescence, flowers and roots compared with the wild-type (WT) under normal growth conditions (Jun et al. 2010; Yamaguchi et al. 2017). These observations suggest that *CLE1–CLE7* regulate plant morphology with a high redundancy.

On the other hand, several studies suggest the involvement of *CLE1–CLE7* peptides in environmental responses. In *Lotus japonicus*, a long distance, root-to-shoot signaling pathway composed of root-derived *LjCLE-ROOT SIGNAL 2* (*CLE-RS2*) and its cognate receptor *HYPERNODULATION ABERRANT ROOT FORMATION 1* (*HAR1*) regulates systemic inhibition of nodulation under excess nitrogen (N) (Okamoto et al. 2009; Yoro et al. 2020). Similarly, in *Arabidopsis*, expression of *CLE1–CLE7*, which are the closest homologs of *LjCLE-RS2*, were affected by nitrate availability in roots (Araya et al. 2014); mRNA levels of *CLE1*, *CLE3*, *CLE4*, and *CLE7* are up-regulated under very low nitrate levels in roots, and overexpression of *CLE1*, *CLE2*, *CLE3*, *CLE4*, and *CLE7* inhibits lateral root growth. Because this growth inhibition is not induced in the *clv1* background, *CLE1–CLE7* are considered to function as mediators that regulate lateral root growth in response to N starvation via the *CLV1*-dependent signaling pathway (Araya et al. 2014).

Because of their sessile nature, plants must coordinate developmental processes according to various environmental stimuli. Recent evidence showed that some CLE peptides other than *CLE1–*

CLE7 mediate the response to environmental stimuli in Arabidopsis. CLE25 peptide expressed in roots acts as a long-distance signal that mediates ABA biosynthesis in leaves and drought stress (Takahashi et al. 2018). CLE9 peptide regulates stomatal closure in response to water deprivation (Zhang et al. 2019). CLE45 peptide protects pollen tube growth under high temperature, which contributes to the maintenance of plant seed production under unfavorable temperature (Endo et al. 2013). Moreover, in *Lotus japonicus*, N level, light availability, and carbohydrate accumulation regulate the expression of *LjCLE-RS2* (Okamoto et al. 2009; Suzuki et al. 2011; Yoro et al. 2020).

In this study, I focused on seven CLE peptides, CLE1–CLE7, to understand their novel function as mediators of different environmental stresses. For this purpose, I examined gene expression profiles of *CLE1–CLE7* in response to different abiotic and biotic stimuli and found that they showed distinctive expression patterns depending on specific stimuli. To know the functions of these peptides, I produced mutants in which the CLE domain was modified using CRISPER/Cas9-based gene editing. By analyzing the mutants, I revealed an indispensable role of *CLE2* in a shade condition. Microarray analyses showed that root-expressed *CLE2* regulates energy metabolism in shoots, which further supported the role of *CLE2* in dark responses. Based on these results, I will discuss the role of *CLE2* in environmental responses.

Chapter II: Materials and methods

Plant materials and vector construction

Plants of *Arabidopsis thaliana* (L.) Heynh. accession Columbia-0 (Col-0) were used as the wild-type (WT). Seeds were surface-sterilized by soaking in 1% (v/v) Plant Preservative Mixture (Plant Cell Technology, Washington, DC, USA) for 1 day at room temperature. Prior to germination, the sterilized seeds were immersed in sterile water and cold-stratified in dark at 4°C for 2 days.

CLE2 sequences were cloned into the Gateway entry vectors (Invitrogen, Carlsbad, CA, USA), according to the manufacturer's instructions. To generate the β -estradiol inducible *CLE2* overexpressing plants (these plants are hereafter referred to as iCLE2 plants), the *CLE2* coding sequence was cloned to the Gateway-compatible *pMDC7* binary vector (Curtis and Grossniklaus 2003) under the control of a G10-90 XVE combined promoter. The upstream and downstream sequences of *CLE2* and *CLE3* were amplified, ligated to the *GUS* coding sequence and cloned into the *pGWB1* vector. The resulting vectors were used to generate transgenic *GUS* reporter lines (Fig. 3D). The *cle2* and *cle3* mutants were generated using the CRISPR/Cas9 system, as described in (Saito et al. 2018). The constructed vectors were introduced into *Agrobacterium tumefaciens* strain GV3101 and used for plant transformation. To genotyping *CLE2* and *CLE3* mutants, I first obtained transformants by bialaphos selection. Then Cas9-free mutants were selected from T₂ population by PCR and sequencing. Primers used for plasmid construction, PCR and sequencing are listed up in Table 1.

GUS reporter analyses

Plants harboring *pCLE2:GUS* or *pCLE3:GUS* were sown on 1/2 MS medium without sucrose and

vertically cultured for 9 days at 22°C under continuous white light ($25\text{--}30\ \mu\text{mol m}^{-2}\ \text{s}^{-1}$). Seedlings were then transplanted into vermiculite (VS kakou, Fukushima, Japan), irrigated with Elix water (Merck Millipore, Burlington, MA, USA), fertilized with HYPONEX 6-10-5 (HYPONEX JAPAN, Osaka, Japan) and grown at 22°C under white light ($45\text{--}50\ \mu\text{mol m}^{-2}\ \text{s}^{-1}$) and 16-h light/8-h dark cycle for 2 weeks. For darkness treatment, seedlings with or without 4 days of dark treatment were prepared. For SA treatment, whole seedling was treated with 1 ml of water (control) or 1 mM NaSA for 24 h. The samples were first placed in 90% acetone and then stained with a GUS staining solution (2 mM X-Gluc, 0.5 mM potassium ferricyanide, 0.5 mM potassium ferrocyanide, and 0.1 M sodium phosphate [pH 7.4]) and washed with 70% ethanol.

Abiotic stress treatments

N depletion treatment

WT seeds were cultured in full nutrition (FN) liquid medium (Scheible et al. 2004) for 5 days at 22°C under continuous white light ($45\text{--}50\ \mu\text{mol m}^{-2}\ \text{s}^{-1}$). These 5-day-old seedlings were then washed and transferred to low nitrogen (–N) medium (Scheible et al. 2004) or FN medium (control). All seedlings were sampled after 3 days.

N replenishment treatment

Five-day-old Arabidopsis seedlings cultured in FN medium were first grown in low N medium for 3 days. Then, the seedlings were supplied with 3 mM KNO₃ or KCl (control) and sampled after 3 h.

Cold treatment

WT seeds were sown in plates containing half-strength Murashige and Skoog (1/2 MS) medium

(Sigma-Aldrich, St. Louis, MO, USA) supplemented with 10 g L⁻¹ sucrose, 0.5 g L⁻¹ 2-morpholinoethanesulfonic acid monohydrate (pH 5.7) and 1% (w/v) Bacto agar (Becton, Dickinson and Company, Franklin Lakes, NJ, USA). The plates were incubated vertically for 10 days at 22°C under continuous white light (25–30 μmol m⁻² s⁻¹). Subsequently, the temperature was decreased to 4°C, and seedlings were sampled after 12 h.

Salt treatment

WT seeds were first sown on 1/2 MS medium and vertically cultured for 10 days at 22°C under continuous white light (25–30 μmol m⁻² s⁻¹). Then, the seedlings were transferred to 1/2 MS medium containing 150 mM NaCl, and incubated roots were sampled after 24 h.

Dark treatment

WT seeds were sown on 1/2 MS medium and vertically cultured for 9 days at 22°C under continuous white light (25–30 μmol m⁻² s⁻¹). Subsequently, the seedlings were wrapped with aluminum foil, and roots and shoots were sampled separately after 48 h.

Sucrose starvation treatment

WT seeds were sown on 1/2 MS medium and vertically cultured at 22°C under continuous white light (25–30 μmol m⁻² s⁻¹) for 9 days. Seedlings were then transferred to 1/2 MS without sucrose, roots were sampled after 48 h.

Shade treatment

WT, *cle2* and *cle3* seeds were sown in vermiculite. The seedlings were irrigated with Elix water,

fertilized with HYPONEX 6-10-5 and grown at 22°C day/20°C night temperature under 16-h light/8-h dark photoperiod using light emitting diodes (LEDs; 65 $\mu\text{mol m}^{-2} \text{s}^{-1}$) until each seedling had four leaves. Seedlings were covered under the insufficient light condition (2 $\mu\text{mol m}^{-2} \text{s}^{-1}$), and grown for 2 weeks.

Quantification of chlorotic phenotype

To quantify the chlorotic level of *cle2* and *cle3* mutant plants, the chlorotic leaf area and the total leaf area of seedlings before and after shade treatment were measured using software ImageJ (National Institutes of Health, Bethesda, MD, USA) and the proportion of chlorotic leaf area was calculated. To quantify the leaf area, the background of the pictures was first colored in black. After which, the total leaf area of a seedling was measured (Hue ≥ 0 ; Saturation ≥ 0 ; Brightness ≥ 80 in HSB color space). Then the chlorotic area was measured ($L^* \geq 175$; $a^* \geq 120$; $b^* \geq 0$ in Lab color space).

Gene expression analysis

Total RNA was isolated from plant tissues using the RNeasy Plant Mini Kit (Qiagen, Hilden, Germany) and used for cDNA synthesis using SuperScript III Reverse Transcriptase (Invitrogen, Waltham, MA, USA) in the presence of RNaseOUT (Invitrogen, Waltham, MA, USA). The cDNA template was used to perform qRT-PCR on the LightCycler480 instrument II (Roche Diagnostics, Basel, Switzerland). Expression levels of *CLE1* (AT1G73165), *CLE2* (AT4G18510), *CLE4* (AT2G31081), *CLE6* (AT2G31085), *CLE7* (AT2G31082), *DIN10* (AT5G20250) and *UBQ10* (AT4G05320) were quantified using TaqMan assays, whereas those of *CLE3* (AT1G06225) and *CLE5* (AT2G31083) were quantified using SYBR Green I assays. *UBQ10* was used as an internal control. Primers used in the analyses were listed up in Table 2.

Microarray analysis

The iCLE2 seedlings carrying the estradiol inducible system were first grown on 1/2 MS medium at 22°C under continuous white light ($25\text{--}30\ \mu\text{mol m}^{-2}\text{ s}^{-1}$) for 7 days. These seedlings were then transferred to 1/2 MS induction medium containing 5 μM β -estradiol or 0.05% DMSO (control) and incubated for 24 h. A parafilm were spread underneath the shoot to prevent contact between shoots and the induction medium. Shoots and roots of seedlings were sampled separately after 24 h and used for microarray analysis, as described previously (Ohashi-Ito et al. 2014). Three biological replicates were performed for each treatment.

Gene ontology (GO) enrichment and gene coexpression analysis

The microarray data were normalized, and genes showing differential expression between the DMSO and β -estradiol treatments ($P < 0.1$; Student's t -test) were selected. GO enrichment analysis was performed on genes showing >1.35 or $<1.35^{-1}$ fold-change in expression following *CLE2* induction using the DAVID Bioinformatics Resources 6.8 (Huang et al. 2009; <https://david.ncifcrf.gov/>). GO terms with $P < 0.01$ in EASE score were shown (Table 3–6).

The top 100 genes up-regulated and down-regulated in shoots and roots were subjected to coexpression analysis using the NetworkDrawer (Ath-m) of database ATTED-II ver. 9.2 (Obayashi et al. 2009; Aoki et al. 2016; <http://atted.jp>). These top 100 genes regulated by *CLE2* were indicated as light gray nodes. Genes coexpressed with at least two of the top 100 genes were indicated as dark gray nodes. Octagonal nodes indicate transcriptional factors.

Chapter III: Results

III-1: Expression of *CLE1–CLE7* in response to abiotic stimuli

To understand the roles of *CLE1–7* peptides in response to various environmental stimuli, I examined the expression levels of the corresponding genes under various conditions such as N depletion, N replenishment, cold, and salt. Because *CLE1–CLE7* are mainly expressed in roots (Jun et al. 2010), I measured the expression levels of these genes in the whole seedling or specifically in roots. In 8-day-old *Arabidopsis* seedlings grown under N depletion condition for 3 days, the expression levels of *CLE2*, *CLE4*, *CLE5*, *CLE6*, and *CLE7* were significantly reduced compared with the control (Fig. 2A). However, exogenous application of potassium nitrate (KNO_3) drastically enhanced the expression levels of *CLE1*, *CLE2*, *CLE4*, *CLE5*, *CLE6*, and *CLE7* in these plants (Fig. 2B). By contrast, N treatments did not affect the expression level of *CLE3*. These data suggest that *CLE1–CLE7* exhibit variation in the response to N availability (Araya et al. 2014). Next, I investigated *CLE* expression levels under cold stress (Fig. 2C). In 10-day-old seedlings exposed to a cold treatment at 4°C for 12 h, the expression of *CLE4*, *CLE5*, *CLE6*, and *CLE7* was significantly up-regulated at 12 h, whereas that of *CLE3* was significantly down-regulated. On the other hand, *CLE1* and *CLE2* showed only a slight increase and no significant change, respectively, in response to cold stress. Finally, I examined salt responsiveness of *CLE* genes. To perform the salt treatment, 10-day-old seedlings were transferred to a medium containing 150 mM NaCl and cultured for 24 h (Fig. 2D). Expression analysis of *CLE* genes in seedling roots showed that *CLE5* was up-regulated, whereas *CLE1*, *CLE2*, *CLE3*, *CLE4*, and *CLE7* were down-regulated. Together, these data indicate that these seven *CLE* genes exhibit different responsiveness to different environmental stimuli, which is inconsistent with the high sequence similarity in the CLE domain.

Plants convert light energy into chemical energy. Therefore, long-term dark treatment is able to affect energy metabolism in plants. To determine if CLE peptides are involved in energy metabolism, I examined expression levels of *CLE* genes in plants grown in the dark for 48 h. Interestingly, the expression of *CLE2* and *CLE3* was up-regulated in roots but not in shoots (Fig. 3A, B). The expression level of a dark inducible marker gene, *DARK INDUCIBLE 10 (DIN10)*, which is reported to reach the maximum transcript level at 24–48 h after the start of dark treatment (Fujiki et al. 2001), was also investigated (Fig. 3A, B). Considering the crosstalk between dark- and sugar starvation-responsive signaling pathways (Baena-González and Sheen 2008; McDowell et al. 2008), I examined *CLE2* and *CLE3* expression levels in response to sucrose starvation. The results showed that the transcript levels of *CLE2* and *CLE3* were increased in the roots of seedlings cultured in medium lacking sucrose for 48 h (Fig. 3C). To investigate the spatial expression pattern of *CLE2* and *CLE3*, I expressed the β -glucuronidase (*GUS*) gene under the control of both the 5' up-stream sequence (promoter) and the 3' down-stream sequence of *CLE2* or *CLE3* gene (*pCLE2:GUS* or *pCLE3:GUS*) (Fig. 3D) in Arabidopsis plants. Under normal growth conditions, GUS staining was observed only in the roots of *pCLE2:GUS* and *pCLE3:GUS* transgenic lines (Fig. 3E, Fig. 4), which is consistent with a previous study (Jun et al. 2010). Close up pictures showed that *pCLE2:GUS* was expressed in the phloem but not in the xylem (Fig. 5, front view), which is in good agreement with the expression pattern on the database Arabidopsis eFP browser (<http://bar.utoronto.ca/efp/cgi-bin/efpWeb.cgi>) that suggests *CLE2* was expressed in phloem and phloem pole pericycle. Moreover, stronger GUS signal was observed in the elongation zone of both the main root and lateral roots in *pCLE2:GUS* plants (Fig. 4, Fig. 5). In contrast, *pCLE3:GUS* signal was observed adjacent to the protoxylem (Fig. 6, side view), which consists with the previous study that showed *CLE3* was expressed in the pericycle (Araya et al. 2014). In addition, *pCLE2:GUS* but not *pCLE3:GUS* was expressed strongly at the

branch and primordia of lateral roots (Fig. 5, Fig. 6). These results suggest that *CLE2* and *CLE3* may have different functions in lateral root development processes. Additionally, a 4-day dark treatment significantly enhanced GUS staining in the root vasculature of both *pCLE2:GUS* and *pCLE3:GUS* plants (Fig. 3E, Fig. 4–6). These results indicate that dark treatment and sucrose starvation induce *CLE2* and *CLE3* expression in roots.

III-2: Function of *CLE2* and *CLE3* in the dark

To determine the function of *CLE2* and *CLE3* peptides, I modified the CLE domain in *CLE2* and *CLE3* using the CRISPR/Cas9 genome editing system (Fig. 7A). Four mutants were generated: *cle2-1*, which carries an 11-nucleotide (nt) deletion in the CLE domain, resulting in a 55-amino acid (aa) peptide in which only the first three amino acid residues match the WT peptide (Fig. 7B); *cle2-2*, which carries a 27-nt deletion, producing a 3-aa peptide; *cle3-2* and *cle3-3*, which carry an additional thymine and adenine, respectively, both resulting in a 7-aa peptide, of which three amino acid residues differ from the WT peptide (Fig. 7B). Each of these four mutants is expected to produce non-functional *CLE2* or *CLE3* peptides because they lack amino acid residues essential for binding to the receptors (Zhang et al. 2016).

Phenotypic analysis of these mutants revealed no visible growth defects in either *cle2* or *cle3* mutant seedlings under normal growth conditions (Fig. 8A). Because *CLE2* and *CLE3* were up-regulated in the dark and in response to sucrose starvation (as shown above), implying that *CLE2* and *CLE3* might contribute to energy metabolism under severe environmental conditions, I examined the phenotype of *cle2* and *cle3* mutant seedlings under dark and sucrose limiting conditions. Although *cle2* and *cle3* seedlings showed no difference in growth compared with the WT when just exposed to dark, the following shade treatment revealed a detectable growth phenotype of *cle2*. Plants were

grown on vermiculite soil supplemented with a N-rich inorganic fertilizer but without any sugar for 2 weeks, and then under shade for another 2 weeks (Fig. 8B). As a result, *cle2-1* and *cle2-2* mutants showed severe chlorosis; however, no such clear phenotype was observed in *cle3-2*, *cle3-3* and WT plants (Fig. 8C, Fig. 9). I quantified the chlorotic levels by measuring the proportion of the chlorotic leaf area using software ImageJ, which confirmed *cle2*-specific chlorosis (Fig. 10).

These results suggest that *CLE2* is involved in the regulation of light-dependent carbohydrate metabolism.

III-3: Downstream components of the CLE2 signaling pathway

To find the downstream components of the *CLE2* signaling pathway, I overexpressed the *CLE2* gene in *Arabidopsis* under the control of an estradiol-inducible promoter; these plants are hereafter referred to as iCLE2 plants. To identify the genes induced by the expression of *CLE2*, the iCLE2 plants were grown for 7 days, and roots were treated with either 5 μ M β -estradiol or DMSO (control) (Fig. 11A). A parafilm was placed underneath the shoots to restrict the estradiol treatment to roots. After 24 h of the estradiol induction, roots and shoots of three biological replicates were sampled separately for RNA extraction. The isolated RNA was used for microarray analysis. Quantitative real-time PCR (qRT-PCR) verified that *CLE2* expression was induced specifically in roots (Fig. 11B).

Based on the results of microarray analysis, genes showing reproducible differences in expression between iCLE2 plants treated with estradiol and DMSO in all three biological replicates ($P < 0.1$) were used for further analysis. Among these, I selected genes up-regulated (fold-change > 1.35) and down-regulated (fold-change $< 1.35^{-1}$) in roots or shoots following the induction of *CLE2* in roots (Fig. 11C). In roots, 295 and 294 genes were up- and down-regulated by *CLE2* induction, respectively (Fig. 11C). Interestingly, although *CLE2* was induced only in roots, 658 and 316 genes

were up- and down-regulated in shoots, respectively (Fig. 11C). Among these genes, only 42 up-regulated and 11 down-regulated genes overlapped between roots and shoots, indicating that many genes were expressed in a root- or shoot-specific manner (Fig. 11C). This result strongly suggests that CLE2 peptides produced in roots regulate gene expression in shoots.

Next, I conducted gene ontology (GO) enrichment analysis of the genes selected above (Table 3, 4). Genes up-regulated in roots were enriched in the following GO terms: ‘response to auxin’, ‘regulation of organ growth’, and ‘auxin-activated signaling pathway’ (Table 3). These GO terms included 12 genes encoding SAUR-like auxin-responsive proteins. Root up-regulated genes also contained genes encoding tRNA and galactose oxidase/kelch repeat superfamily proteins (Table 3). Additionally, genes down-regulated in roots were enriched in the following GO terms: ‘hypoxia response’, ‘oxidative stress response’, ‘defense response’, ‘thalianol metabolic process’ and ‘cytokinin catabolic process’ (Table 3).

In shoots, the up-regulated genes were enriched in the following GO terms: ‘response to chitin’, ‘response to salicylic acid’, ‘defense response’, ‘proteasome-mediated ubiquitin-dependent protein catabolic process’, ‘carbohydrate metabolic process’, ‘regulation of phenylpropanoid metabolic process’, and ‘trehalose metabolism in response to stress’ (Table 4). Three galactose oxidase/kelch repeat superfamily protein genes were up-regulated in shoots as well as roots. Additionally, genes down-regulated in shoots were enriched in the following GO terms: ‘defense response to fungus’, ‘killing of cells of other organism’, ‘glucosinolate biosynthetic process’, and ‘lipid transport’ (which included defensin-like genes and lipid transport proteins) (Table 4).

To identify *CLE2*-related genes, I conducted an association analysis using the top 100 genes up-regulated and down-regulated in shoots and roots (Table 5–9; Fig. 12–15), based on the ATTED-II database (<http://atted.jp>; Obayashi et al. 2009; Aoki et al. 2016). The top 100 genes are shown as

light gray nodes, and the coexpressing genes, which showed associations with at least two light gray node genes in the ATTED-II database, are indicated as dark gray nodes. Dark gray nodes labeled with asterisks represent genes up- or down-regulated by *CLE2* but not included among the top 100 genes. The results of this association analysis revealed four coexpression networks comprising genes up-regulated in shoots. The largest network consisted of 39 light gray nodes and 28 dark gray nodes, of which 19 were labeled with asterisks, indicating that these genes are also up-regulated by *CLE2*. This shows that *CLE2* induced the expression of a large set of genes including a gene encoding the beta subunit of SnRK1 (*AKINBETA1*), three dark-inducible genes (*DIN1*, *DIN6*, and *DIN10*), a key autophagy gene (*ATG8E*) and a group of trehalose-6-phosphate (T6P) phosphatase/synthase genes (*TPS8*, *TPS9*, and *TPS11*) (Fig. 12). On the other hand, genes down-regulated in shoots, up-regulated in roots, or down-regulated in roots formed more disperse and small networks (Fig. 13–15). These small networks contained lipid transfer protein family genes (down-regulated in shoots) (Fig. 13), SAUR-like auxin responsive genes (up-regulated in roots) (Fig. 14), and thalianol metabolism-related genes (*THAS1*, *THAH1* and *THAD1*; down-regulated in roots) (Fig. 15).

Overall, genes up-regulated by *CLE2* in shoots formed a condensed SnRK1-related coexpression network, which strongly supports the indispensability of *CLE2* in dark responses. In addition, *CLE2* expression in roots induced multiple transcriptional events in roots and shoots within 24 h, which is in agreement with the function of CLEs as plant signaling peptides.

Chapter IV: Discussion

IV-1: Expression profiles of *CLE1–CLE7* in response to different environmental stimuli

To understand the function of *CLE1–CLE7* as mediators of environmental stimuli, I first studied the expression profiles of these genes in response to various environmental stimuli including N depletion, N replenishment, cold, salt, and dark. The *CLE1–CLE7* genes share high sequence similarity in the CLE domain and therefore similar functions (Fig. 1). A previous study reported that nitrate application suppressed the expression of *CLE1*, *CLE3*, *CLE4*, and *CLE7* but not that of *CLE2* and *CLE5* (Araya et al. 2014). In this dissertation, I further analyzed the responsiveness of these *CLE* genes to nitrate depletion and replenishment. The results showed that most *CLE* genes, except *CLE3*, were down-regulated by N depletion and up-regulated by N replenishment (Fig. 2A, B). These results indicate that *CLE1–CLE7* exhibit differential but fine-tuned response to subtle changes in N levels. Further analysis revealed that *CLE1–CLE7* are also responsive to other environmental stimuli such as cold, salt, and light (Fig. 2C, D; Fig. 3A, B). Compared with *CLE4–CLE7*, *CLE3* showed an opposite response to cold stress (Fig. 2C). On the other hand, among *CLE1–CLE7*, only *CLE5* was up-regulated by salt stress (Fig. 2D). Moreover, *CLE1*, *CLE3* and *CLE4* were induced by flg22 treatment (Fig. 16A), while *CLE3* alone was also induced by Pep2 and NaSA treatment (Fig. 16B, D). These results suggest that *CLE1–CLE7* peptides may mediate different environmental stimuli in a distinct manner, probably with some redundancy. Members of these CLE genes respond to same environmental stimuli may have redundant functions, which brings plants robust responses upon different environmental stimuli. On the other hand, CLE genes that specifically respond to certain stimuli may harbor specific functions. For example, *CLE3* may specifically function in immune responses (Fig. 16), while *CLE5* may have specific role in salt stress responses (Fig. 2D). These responsive differences of *CLE1–CLE7* could finally result in the functional diversity.

IV-2: Functions of CLE2 peptide

To understand the role of CLE peptides in mediating environmental stimuli in further detail, I first analyzed the spatial expression patterns, gene regulatory network and mutant phenotype of *CLE* genes, with a special focus on *CLE2*. Microarray analysis revealed that root-specific *CLE2* overexpression altered the expression levels of many genes in roots. The most striking change was the induction of a group of auxin-inducible *SAUR* genes. Previous study indicated that *CLE2* overexpression suppresses lateral root growth (Araya et al. 2014), which is regulated by auxin. These data suggest that CLE2 signaling is somehow associated with auxin signaling in roots.

Importantly, although *CLE2* was overexpressed only in roots, the expression of many genes was altered in shoots, suggesting that the CLE2 peptide itself or a CLE2-induced factor(s) moves from roots to shoots to regulate gene expression. Because a previous report indicates that CLE6 moves from roots to shoots to regulate GA-dependent shoot growth (Bidadi et al. 2014), CLE2 may also move to shoots to function systemically. *CLE2* was up-regulated by N replenishment, dark, and sugar starvation (Fig. 2B, Fig. 3A, C). To understand the function of *CLE2* and *CLE3* at the genetic level, I generated *cle2* and *cle3* mutants using the CRISPR/Cas9 system; these mutants did not produce functional CLE2 or CLE3 peptides (Fig. 7). The *cle2* mutants showed a severe growth defect with chlorosis under conditions of high N, no sugar, and low light (Fig. 8C, Fig. 9). By contrast, *cle3* plants showed no such obvious growth phenotype under the same condition (Fig. 8C, Fig. 9), although the CLE domains of CLE2 and CLE3 differed by only a single amino acid (Fig. 1), and *CLE3* was also up-regulated in response to dark and sugar starvation (Fig. 3A, C), like *CLE2*. Recent studies demonstrate that CLE25 and CLE26 differently move from roots to shoots and CLE25, but not CLE26, induces an ABA biosynthesis gene in shoots (Takahashi et al. 2018; Endo et al. 2019),

although there is only a single amino acid difference between the two peptides. Therefore, differences in the transport activity and function of CLE2 and CLE3 may affect the phenotypic differences between *cle2* and *cle3* mutants.

In this study, I found that root-specific *CLE2* overexpression significantly induced several dark-inducible genes such as *DIN1* (*SEN1*), *DIN4*, *DIN6* (*ASNI*), and *DIN10* (*RS6*) in the shoots (Table 5, Fig. 12). *CLE2* overexpression in roots also increased the expression of various genes in shoots, including genes encoding the beta subunits of SnRK1 (*AKINBETA1*) and those encoding T6P phosphatase/synthase enzymes (*TPS8*, *TPS9*, and *TPS11*) (Table 5, Fig. 12). In the natural environment, insufficient light due to shading by surrounding plants affects photosynthetic sugar production (Baena-González and Sheen 2008; McDowell et al. 2008). SnRK1, a widely conserved kinase complex, acts as a metabolic sensor that adjusts the plant metabolism according to the energy demand and functions as a central component of the stress and energy signaling machinery in *Arabidopsis* (Polge and Thomas 2006). TPS8–11 regulate the level of T6P, which regulates carbohydrate metabolism as well as plant growth and development (Ramon and Rolland 2007). These results suggest that *CLE2* regulates carbohydrate metabolism at the transcriptional level under low sugar and shade conditions; this is consistent with the phenotype of *cle2* mutant plants. Taken together, this study suggests that CLE2 mediates *in situ* carbon metabolism under poor energy environment.

I found that *CLE2* expression is induced in roots, which is probably regulated by photoassimilates derived from shoots in response to different light conditions. The results also indicated that *CLE2* induction in roots was capable of modulating the expression of dark responsive metabolic genes in shoots. Thus, the CLE2-involved shoot–root–shoot signaling may occur for integrating light-dependent carbon metabolic status in roots and conducting appropriate overall

systemic responses from roots to shoots. Although the direction is opposite, root–shoot–root signaling via root-derived peptides such as LjCLE-RS2 and C-TERMINALLY ENCODED PEPTIDE 1 regulates overall systemic nitrogen assimilation-dependent responses (Okamoto et al. 2009; Tabata et al. 2014). Further efforts will be made for better understanding this signaling mechanism, which could also facilitate us to understand how plants survive the changing environment.

In conclusion, in this study, I shed light on the functional diversity of *CLE1–CLE7* genes as mediators of environmental stimuli, focusing on functional specificity of *CLE2*. By using these *CLE* genes, plants can respond to different environmental stimuli more robustly and cost-effectively, which would confer them the capacity to survive harsh environments.

Table 1. Primers used in mutant preparation

Primer	Sequence (5'→3')	Objective
CLE2cds-cacc-F	CACCATGGCTAAGTTAAGCTTCACTTTCT	For iCLE2
CLE2cds-R	CTAGTGATGTTGTGGGTCGG	
CLE2-upstream(2.2kb)-cacc-F	CACCTAGCATTTCATATACCACACAAGATTTATTT	For pCLE2:GUS
CLE2-downstream(2.8kb)-R	GCCAATGCAAGAATTTTAATGATGACCAATTATATCTATTAA	
CLE3-upstream(3.2kb)-cacc-F	CACCGTATCTAATTGTATCTCTAATTTGGCT	For pCLE3:GUS
CLE3-downstream(1.4kb)-R	ACATATACTTCAGAAACCCTAATTTACGC	
CLE2(184–206)CRISPR A	ATTGCCAGAGCGGTTAAGCCCAGG	For cle2
CLE2(184–206)CRISPR B	AAACCCTGGGCTTAACCGCTCTGG	
CLE3(208–230)CRISPR A	ATTGTCAAAGCGGCTTAGTCCCGG	For cle3
CLE3(208–230)CRISPR B	AAACCCGGGACTAAGCCGCTTTGA	
CLE2-up-F	CACTTGCTCAGCTGGTTACAGATTAAATAT	PCR of cle2 genotyping
CLE2-down-R2	CATACGTACCGCGTTGCTATAG	PCR of cle2 genotyping
CLE2-down-R1	TCACCAAATTTAGAATATTTAGTTAACGTAC	Sequencing of cle2 genotyping
CLE3-up-F	GACTAGATTCCAACCTTAATTAACGTATTTA	PCR of cle3 genotyping
CLE3-down-R2	GAACTACATAAAAACGAGATCATGTAAACAG	PCR of cle3 genotyping
CLE3-down-R1	TTGTAATATCATATTAAACTCTCCCAAAA	Sequencing of cle3 genotyping

Table 2. Primers used in qRT-PCR

Primer	Sequence (5'→3')	Probe
CLE1-Taq-F	GGATTAAACGAGGGCGTATG	#6
CLE1-Taq-R	GCTTCTCCATACTCGCTTTCA	
CLE2-Taq-F	TGTTTCTTCTGTTATCCTC	#11
CLE2-Taq-R	GCTTAGGCCTCTCACCTTC	
CLE4-Taq-F	CGAGTTCTCGGTGCATCA	#164
CLE4-Taq-R	CCTGAATCTGAAGGGCTCTCT	
CLE6-Taq-F	TCTCAATCTCTTAAGATCCCACAA	#143
CLE6-Taq-R	CTTAAGGATCAAATTCGCCATT	
CLE7-Taq-F	TTCCGTCCAAAACGAAGTAGA	#80
CLE7-Taq-R	AGAGTGATGTTGAGGGTCAGG	
UBQ10-Taq-F	GAAGTTCAATGTTTCGTTTCATGT	#119
UBQ10-Taq-R	GGATTATACAAGGCCCAAAA	
DIN10-Taq-F	GGTGGGCCTCTCTATGTCA	#2
DIN10-Taq-R	CCATCAGGCAATACAAGCTTTC	
CLE3-SYBR-F	GACTAGTGCTTCTAGTACTCGAATTGA	
CLE3-SYBR-R	TCAGTGATGCCTCGGGTC	
CLE5-SYBR-F	ACTCCCACCCCTCCAAATTCA	
CLE5-SYBR-R	CTATCCATATTGCCCATGGACAC	

Table 3. GO enrichment analysis of *CLE2* up- and down-regulated genes in roots

Term ^a	<i>P</i> -value	Fold change
Up-regulated genes		
Response to auxin	3.50E-08	6.3
Regulation of organ growth	1.30E-04	38.3
Auxin-activated signaling pathway	2.50E-04	5.4
Translational elongation	1.20E-03	2.6
Regulation of phenylpropanoid metabolic process	1.50E-03	49.2
Down-regulated genes		
Cellular response to hypoxia	2.20E-04	16.4
Oxidation-reduction process	3.90E-04	2
Thalianol metabolic process	4.00E-04	85.2
Response to oxidative stress	6.50E-04	3.5
Secondary metabolite biosynthetic process	1.60E-03	4.7
Cytokinin catabolic process	2.70E-03	36.5
Hydrogen peroxide catabolic process	3.90E-03	5.7
Plant-type cell wall organization	4.30E-03	5.6
Defense response	4.60E-03	2.2
Response to toxic substance	5.60E-03	7

^aThe selected GO terms showed significant EASE scores ($P < 0.01$).

Table 4. GO enrichment analysis of *CLE2* up- and down-regulated genes in shoots

Term ^a	<i>P</i> -value	Fold change
Up-regulated		
Response to chitin	4.70E-04	4
Response to salicylic acid	1.50E-03	3.4
Regulation of transcription, DNA-templated	2.30E-03	1.4
Defense response	5.80E-03	1.8
Proteasome-mediated ubiquitin-dependent protein catabolic process	7.70E-03	2.4
Carbohydrate metabolic process	7.90E-03	2.1
Regulation of phenylpropanoid metabolic process	8.50E-03	20.5
Trehalose metabolism in response to stress	9.00E-03	9.1
Down-regulated		
Defense response to fungus	8.00E-04	2.9
Killing of cells of other organism	1.60E-03	3.4
Lipid transport	7.00E-03	4.1
Glucosinolate biosynthetic process	7.60E-03	9.8

^aThe selected GO terms showed significant EASE scores ($P < 0.01$).

Table 5. *CLE2* up-regulated top 100 genes in shoots

AGI code	Gene	Fold change	P-value	Description
AT3G58910	---	3.43	0.04	F-box family protein
AT4G15660	---	3.37	0.07	Thioredoxin superfamily protein
AT5G56870	BGAL4	3.26	0.03	beta-galactosidase 4
AT2G44130	KMD3	3.18	0.00	Galactose oxidase/kelch repeat superfamily protein
AT4G35770	SEN1/DIN1	2.82	0.07	Rhodanese/Cell cycle control phosphatase superfamily protein
AT3G48360	BT2	2.77	0.00	BTB and TAZ domain protein 2
AT4G27450	---	2.76	0.02	Aluminium induced protein with YGL and LRDR motifs
AT3G15450	---	2.72	0.01	Aluminium induced protein with YGL and LRDR motifs
AT3G20395	---	2.67	0.07	RING/U-box superfamily protein
AT3G47340	ASN1/DIN6	2.60	0.09	glutamine-dependent asparagine synthase 1
AT2G18700	TPS11	2.60	0.06	trehalose phosphatase/synthase 11
AT3G61060	PP2-A13	2.56	0.01	phloem protein 2-A13
AT1G26240	---	2.51	0.07	Proline-rich extensin-like family protein
AT4G10910	---	2.49	0.00	---
AT3G24290	---	2.48	0.09	ammonium transporter 1;5
AT5G48850	ATSDI1	2.48	0.05	Tetratricopeptide repeat (TPR)-like superfamily protein
AT4G24230	ACBP3	2.45	0.00	acyl-CoA-binding domain 3
AT5G19120	---	2.44	0.00	Eukaryotic aspartyl protease family protein
AT1G02610	---	2.44	0.09	RING/FYVE/PHD zinc finger superfamily protein
AT1G10140	---	2.44	0.05	Uncharacterised conserved protein UCP031279
AT2G15880	---	2.44	0.02	Leucine-rich repeat (LRR) family protein
AT4G35640	---	2.44	0.00	serine acetyltransferase 3;2
AT1G80440	---	2.39	0.00	Galactose oxidase/kelch repeat superfamily protein
AT2G20670	---	2.38	0.00	Protein of unknown function (DUF506)
AT2G40000	HSPRO2	2.36	0.00	ortholog of sugar beet HS1 PRO-1 2
AT4G37610	BT5	2.35	0.00	BTB and TAZ domain protein 5
AT5G26220	---	2.33	0.04	ChaC-like family protein
AT3G07350	---	2.31	0.00	Protein of unknown function (DUF506)
AT5G18130	---	2.28	0.00	---
AT1G36060	---	2.24	0.01	Integrase-type DNA-binding superfamily protein
AT2G17880	---	2.24	0.03	Chaperone DnaJ-domain superfamily protein
AT4G32480	---	2.23	0.00	Protein of unknown function (DUF506)
AT5G55970	---	2.19	0.00	RING/U-box superfamily protein
AT1G28330	DYL1	2.19	0.01	dormancy-associated protein-like 1
AT3G15630	---	2.19	0.02	---
AT1G75490	---	2.17	0.02	Integrase-type DNA-binding superfamily protein
AT5G02020	---	2.16	0.01	---
AT4G38825	SAUR13	2.16	0.05	SAUR-like auxin-responsive protein family
AT5G22920	---	2.14	0.01	CHY-type/CTCHY-type/RING-type Zinc finger protein
AT5G44260	---	2.14	0.06	Zinc finger C-x8-C-x5-C-x3-H type family protein
AT4G36850	---	2.14	0.01	PQ-loop repeat family protein / transmembrane family protein
AT5G03820	---	2.13	0.05	GDSL-like Lipase/Acylhydrolase family protein
AT5G56550	OXS3	2.12	0.00	oxidative stress 3
AT3G63088	RTFL14	2.12	0.00	ROTUNDIFOLIA like 14
AT3G20340	---	2.12	0.02	---
AT5G55110	---	2.10	0.06	Stigma-specific Stig1 family protein
AT1G17147	---	2.09	0.00	VQ motif-containing protein
AT4G26288	---	2.08	0.03	---
AT5G63160	BT1	2.07	0.01	BTB and TAZ domain protein 1
AT4G26290	---	2.07	0.00	---

Table 5. (Continued.)

AGI code	Gene	Fold change	P-value	Description
AT5G43200	---	2.06	0.06	Zinc finger, C3HC4 type (RING finger) family protein
AT2G25900	---	2.05	0.02	Zinc finger C-x8-C-x5-C-x3-H type family protein
AT4G21510	---	2.04	0.00	F-box family protein
AT1G06120	---	2.02	0.03	Fatty acid desaturase family protein
AT1G04770	---	2.01	0.01	Tetratricopeptide repeat (TPR)-like superfamily protein
AT3G45860	CRK4	2.01	0.06	cysteine-rich RLK (RECEPTOR-like protein kinase) 4
AT2G24550	---	2.00	0.01	---
AT3G15440	---	2.00	0.02	---
AT5G36190	---	2.00	0.00	---
AT1G66280	---	1.99	0.08	Glycosyl hydrolase superfamily protein
AT5G20250	DIN10	1.98	0.07	Raffinose synthase family protein
AT3G23470	---	1.97	0.01	Cyclopropane-fatty-acyl-phospholipid synthase
AT4G11250	AGL52	1.97	0.09	AGAMOUS-like 52
AT1G49130	---	1.97	0.00	B-box type zinc finger protein with CCT domain
AT1G03850	---	1.97	0.04	Glutaredoxin family protein
AT5G63590	FLS3	1.94	0.02	flavonol synthase 3
AT2G24240	---	1.94	0.03	BTB/POZ domain with WD40/YVTN repeat-like protein
AT4G08895	---	1.93	0.02	inorganic phosphate transporter family protein
AT3G62950	---	1.92	0.08	Thioredoxin superfamily protein
AT5G18870	---	1.92	0.09	Inosine-uridine preferring nucleoside hydrolase family protein
AT1G11593	---	1.92	0.08	Plant invertase/pectin methylesterase inhibitor superfamily protein
AT2G15460	---	1.92	0.01	Pectin lyase-like superfamily protein
AT5G21940	---	1.92	0.00	---
AT5G59090	SBT4.12	1.91	0.01	subtilase 4.12
AT2G38820	---	1.91	0.00	Protein of unknown function (DUF506)
AT3G15500	NAC3	1.90	0.06	NAC domain containing protein 3
AT5G14130	---	1.90	0.00	Peroxidase superfamily protein
AT1G23870	TPS9	1.90	0.02	trehalose-phosphatase/synthase 9
AT4G15670	---	1.90	0.08	Thioredoxin superfamily protein
AT3G10020	---	1.89	0.00	---
AT1G23390	---	1.89	0.00	Kelch repeat-containing F-box family protein
AT5G42260	BGLU12	1.89	0.00	beta glucosidase 12
AT3G21460	---	1.89	0.00	Glutaredoxin family protein
AT5G38370	---	1.88	0.07	Protein of unknown function (DUF1644)
AT2G16220	---	1.88	0.07	F-box and associated interaction domains-containing protein
AT1G03090	MCCA	1.88	0.04	methylcrotonyl-CoA carboxylase alpha chain, mitochondrial / 3-methylcrotonyl-CoA carboxylase 1 (MCCA)
AT1G02660	---	1.87	0.08	alpha/beta-Hydrolases superfamily protein
AT3G59590	---	1.87	0.00	jacalin lectin family protein
AT5G16023	RTFL18	1.86	0.02	ROTUNDIFOLIA like 18
AT1G22370	UGT85A5	1.86	0.00	UDP-glucosyl transferase 85A5
AT5G08315	---	1.86	0.07	Defensin-like (DEFL) family protein
AT5G56470	---	1.85	0.02	FAD-dependent oxidoreductase family protein
AT2G02710	PLPB	1.85	0.00	PAS/LOV protein B
AT1G70290	TPS8	1.85	0.02	trehalose-6-phosphatase synthase S8
AT1G80920	---	1.84	0.01	Chaperone DnaJ-domain superfamily protein
AT1G27260	---	1.84	0.02	Paired amphipathic helix (PAH2) superfamily protein
AT5G21170	AKINBETA1	1.84	0.03	5'-AMP-activated protein kinase beta-2 subunit protein
AT5G57550	XTH25	1.84	0.05	xyloglucan endotransglucosylase/hydrolase 25
AT4G38820	---	1.83	0.05	---
AT2G28850	CYP710A3	1.83	0.09	cytochrome P450, family 710, subfamily A, polypeptide 3

Table 6. *CLE2* down-regulated top 100 genes in shoots

AGI code	Gene	Fold change	P-value	Description
AT5G59310	LTP4	0.06	0.09	lipid transfer protein 4
AT5G59320	LTP3	0.17	0.05	lipid transfer protein 3
AT2G35070	---	0.43	0.01	---
AT3G22600	---	0.43	0.01	Bifunctional inhibitor/lipid-transfer protein/seed storage 2S albumin superfamily protein
AT2G37870	---	0.43	0.03	Bifunctional inhibitor/lipid-transfer protein/seed storage 2S albumin superfamily protein
AT3G09450	---	0.44	0.01	---
AT2G03300	---	0.45	0.02	Toll-Interleukin-Resistance (TIR) domain family protein
AT3G27510	---	0.45	0.07	Cysteine/Histidine-rich C1 domain family protein
AT3G47675	---	0.47	0.08	---
AT4G12480	---	0.49	0.05	Bifunctional inhibitor/lipid-transfer protein/seed storage 2S albumin superfamily protein
AT3G53980	---	0.50	0.01	Bifunctional inhibitor/lipid-transfer protein/seed storage 2S albumin superfamily protein
AT5G23180	---	0.50	0.08	---
AT5G37250	---	0.51	0.01	RING/U-box superfamily protein
AT1G77870	MUB5	0.51	0.06	membrane-anchored ubiquitin-fold protein 5 precursor
AT2G24625	---	0.53	0.07	Defensin-like (DEFL) family protein
AT5G53230	DUF295	0.54	0.04	Protein of unknown function (DUF295)
AT4G11911	---	0.54	0.07	---
AT2G34825	RALFL20	0.54	0.04	RALF-like 20
AT4G13800	DUF803	0.54	0.04	Protein of unknown function (DUF803)
AT3G22231	PCC1	0.55	0.01	pathogen and circadian controlled 1
AT5G60890	MYB34	0.56	0.08	myb domain protein 34
AT2G42540	COR15A	0.56	0.01	cold-regulated 15a
AT1G09483	---	0.56	0.09	---
AT5G05340	---	0.56	0.05	Peroxidase superfamily protein
AT1G69100	---	0.57	0.02	Eukaryotic aspartyl protease family protein
AT5G13170	SAG29	0.57	0.01	senescence-associated gene 29
AT4G01671	---	0.58	0.09	---
AT1G20070	---	0.58	0.01	---
AT3G23110	RLP37	0.58	0.02	receptor like protein 37
AT3G23120	RLP38	0.58	0.00	receptor like protein 38
AT1G61600	DUF1262	0.58	0.02	Protein of unknown function (DUF1262)
AT5G07010	ST2A	0.59	0.09	sulfotransferase 2A
AT1G76530	---	0.59	0.08	Auxin efflux carrier family protein
AT1G65300	AGL38	0.60	0.08	AGAMOUS-like 38
AT5G38760	---	0.60	0.08	Late embryogenesis abundant protein (LEA) family protein
AT5G26250	---	0.60	0.03	Major facilitator superfamily protein
AT5G56010	HSP81-3	0.61	0.01	heat shock protein 81-3
AT4G10720	---	0.61	0.03	Ankyrin repeat family protein
AT3G12060	TBL1	0.61	0.03	Plant protein of unknown function (DUF828)
AT2G19045	RALFL13	0.61	0.01	RALF-like 13
AT3G01070	ENODL16	0.61	0.00	early nodulin-like protein 16
AT3G50890	HB28	0.61	0.01	homeobox protein 28
AT1G03743	---	0.61	0.01	snoRNA
AT1G78206	---	0.61	0.09	MIR775a; miRNA
AT1G26410	---	0.61	0.02	FAD-binding Berberine family protein
AT1G63560	---	0.61	0.07	Receptor-like protein kinase-related family protein
AT4G09590	NHL22	0.62	0.08	NDR1/HIN1-like 22
AT4G14276	---	0.62	0.03	Defensin-like (DEFL) family protein
AT2G46870	NGA1	0.62	0.06	AP2/B3-like transcriptional factor family protein

Table 6. (Continued.)

AGI code	Gene	Fold change	P-value	Description
AT3G27720	ARI4	0.62	0.07	IBR domain containing protein
AT4G01703	---	0.62	0.00	---
AT3G09620	---	0.63	0.08	P-loop containing nucleoside triphosphate hydrolases superfamily protein
AT5G46700	TRN2	0.63	0.02	Tetraspanin family protein
AT2G01740	---	0.63	0.00	Tetratricopeptide repeat (TPR)-like superfamily protein
AT1G65350	UBQ13	0.63	0.06	ubiquitin 13
AT3G17790	PAP17	0.63	0.05	purple acid phosphatase 17
AT1G63190	---	0.63	0.06	Cystatin/monellin superfamily protein
AT2G44940	---	0.63	0.04	Integrase-type DNA-binding superfamily protein
AT1G70230	TBL27	0.63	0.00	TRICHOME BIREFRINGENCE-LIKE 27
AT5G15110	---	0.63	0.02	Pectate lyase family protein
AT4G25885	---	0.63	0.01	other RNA
AT5G49270	SHV2	0.64	0.06	COBRA-like extracellular glycosyl-phosphatidyl inositol-anchored protein family
AT3G06545	---	0.64	0.04	---
AT4G36160	NAC076	0.64	0.02	NAC domain containing protein 76
AT1G11112	---	0.64	0.06	---
AT4G30030	---	0.64	0.01	Eukaryotic aspartyl protease family protein
AT1G10000	---	0.64	0.02	Ribonuclease H-like superfamily protein
AT3G20460	---	0.64	0.00	Major facilitator superfamily protein
AT3G29790	---	0.64	0.09	---
AT2G36815	---	0.64	0.07	---
AT3G43574	---	0.64	0.04	---
AT3G11825	---	0.64	0.02	Bifunctional inhibitor/lipid-transfer protein/seed storage 2S albumin superfamily protein
AT1G56670	---	0.64	0.02	GDSL-like Lipase/Acylhydrolase superfamily protein
AT5G03350	---	0.65	0.03	Legume lectin family protein
AT4G08360	---	0.65	0.00	KOW domain-containing protein
AT2G25940	ALPHA-VPE	0.65	0.07	alpha-vacuolar processing enzyme
AT3G60140	DIN2	0.65	0.01	Glycosyl hydrolase superfamily protein
AT1G66830	---	0.65	0.03	Leucine-rich repeat protein kinase family protein
AT1G65860	FMO GS-OX1	0.65	0.01	flavin-monooxygenase glucosinolate S-oxygenase 1
AT1G31163	---	0.65	0.01	F-box associated ubiquitination effector family protein
AT1G48605	---	0.65	0.04	Flavoprotein
AT1G52070	---	0.65	0.01	Mannose-binding lectin superfamily protein
AT4G15248	---	0.65	0.09	B-box type zinc finger family protein
AT2G16760	---	0.65	0.01	Calcium-dependent phosphotriesterase superfamily protein
AT5G15430	---	0.65	0.04	Plant calmodulin-binding protein-related
AT5G54060	UF3GT	0.65	0.06	UDP-glucose:flavonoid 3-o-glucosyltransferase
AT5G67620	---	0.65	0.06	---
AT1G36000	LBD5	0.65	0.05	LOB domain-containing protein 5
AT4G29033	---	0.65	0.06	Defensin-like (DEFL) family protein
AT2G46280	TRIP-1	0.65	0.01	TGF-beta receptor interacting protein 1
AT1G26210	SOFL1	0.65	0.01	SOB five-like 1
AT1G55610	BRL1	0.66	0.00	BRI1 like
AT1G76240	DUF241	0.66	0.09	Arabidopsis protein of unknown function (DUF241)
AT3G48320	CYP71A21	0.66	0.02	cytochrome P450, family 71, subfamily A, polypeptide 21
AT3G26125	CYP86C2	0.66	0.01	cytochrome P450, family 86, subfamily C, polypeptide 2
AT1G51770	---	0.66	0.04	Core-2/I-branching beta-1,6-N-acetylglucosaminyltransferase family protein
AT5G39380	---	0.66	0.06	Plant calmodulin-binding protein-related
AT3G45450	---	0.66	0.04	Double Clp-N motif-containing P-loop nucleoside triphosphate hydrolases superfamily protein
AT1G53543	---	0.66	0.05	---
AT4G14700	ORC1A	0.66	0.00	origin recognition complex 1

Table 7. *CLE2* up-regulated top 100 genes in roots

AGI code	Gene	Fold change	P-value	Description
AT5G18030	SAUR21	4.56	0.02	SAUR-like auxin-responsive protein family
AT5G18080	SAUR24	2.94	0.00	SAUR-like auxin-responsive protein family
AT5G18020	SAUR20	2.64	0.01	SAUR-like auxin-responsive protein family
AT5G18010	SAUR19	2.49	0.05	SAUR-like auxin-responsive protein family
AT4G38825	SAUR13	2.23	0.02	SAUR-like auxin-responsive protein family
AT2G21740	DUF1278	2.15	0.01	Protein of unknown function (DUF1278)
AT1G80440	KMD1	2.00	0.00	Galactose oxidase/kelch repeat superfamily protein
AT5G56550	OXS3	1.96	0.04	oxidative stress 3
AT4G31196	---	1.93	0.04	oxidoreductases
AT2G44130	KMD3	1.90	0.02	Galactose oxidase/kelch repeat superfamily protein
AT4G00651	---	1.89	0.04	---
AT3G48360	BT2	1.88	0.07	BTB and TAZ domain protein 2
AT3G03820	SAUR29	1.82	0.01	SAUR-like auxin-responsive protein family
AT2G15880	---	1.79	0.03	Leucine-rich repeat (LRR) family protein
AT1G29510	SAUR68	1.79	0.04	SAUR-like auxin-responsive protein family
AT3G20360	---	1.78	0.01	TRAF-like family protein
AT4G38820	---	1.78	0.00	---
AT1G76410	---	1.76	0.05	RING/U-box superfamily protein
AT3G60470	DUF247	1.76	0.07	Plant protein of unknown function (DUF247)
AT5G37560	---	1.76	0.05	RING/U-box superfamily protein
AT5G03090	---	1.74	0.03	---
AT5G49152	---	1.73	0.04	other RNA
AT4G38840	SAUR14	1.73	0.06	SAUR-like auxin-responsive protein family
AT3G13310	---	1.73	0.00	Chaperone DnaJ-domain superfamily protein
AT5G41280	---	1.71	0.05	Receptor-like protein kinase-related family protein
AT1G32720	---	1.70	0.00	Cytochrome C oxidase polypeptide VIB family protein
AT1G29500	SAUR66	1.70	0.08	SAUR-like auxin-responsive protein family
AT1G50603	---	1.69	0.07	---
AT1G31163	---	1.68	0.01	F-box associated ubiquitination effector family protein
AT4G28580	MGT5	1.66	0.02	magnesium transport 5
AT4G17245	---	1.66	0.01	RING/U-box superfamily protein
AT1G26800	---	1.65	0.02	RING/U-box superfamily protein
AT1G13245	RTFL17	1.65	0.00	ROTUNDIFOLIA like 17
AT1G21245	---	1.62	0.07	Protein kinase superfamily protein
AT1G24070	CSLA10	1.60	0.04	cellulose synthase-like A10
AT5G45450	---	1.59	0.03	Oligopeptide transporter OPT superfamily protein
AT4G24230	ACBP3	1.59	0.09	acyl-CoA-binding domain 3
AT3G44180	---	1.59	0.03	syntxin-related family protein
AT2G45135	---	1.58	0.01	RING/U-box superfamily protein
AT5G28090	---	1.58	0.05	---
AT2G46493	---	1.58	0.05	RING/U-box superfamily protein
AT5G39750	AGL81	1.58	0.02	AGAMOUS-like 81
AT5G39390	---	1.58	0.07	Leucine-rich repeat protein kinase family protein
AT1G29450	SAUR64	1.58	0.01	SAUR-like auxin-responsive protein family
AT5G54585	---	1.58	0.07	---
AT1G50780	---	1.57	0.06	2Fe-2S ferredoxin-like superfamily protein
AT5G41380	---	1.57	0.05	CCT motif family protein
AT4G19035	LCR7	1.57	0.02	low-molecular-weight cysteine-rich 7
AT4G36280	---	1.57	0.05	Histidine kinase-, DNA gyrase B-, and HSP90-like ATPase family protein
AT2G47120	---	1.57	0.03	NAD(P)-binding Rossmann-fold superfamily protein

Table 7. (Continued.)

AGI code	Gene	Fold change	P-value	Description
AT5G59080	---	1.56	0.01	---
AT1G12451	---	1.56	0.07	---
AT5G24550	BGLU32	1.56	0.04	beta glucosidase 32
AT3G13594	---	1.56	0.07	---
AT4G16515	RGF6	1.56	0.04	---
AT3G18773	---	1.56	0.05	RING/U-box superfamily protein
AT1G02490	---	1.56	0.06	---
AT4G20990	ACA4	1.56	0.06	alpha carbonic anhydrase 4
AT5G61590	---	1.55	0.07	Integrase-type DNA-binding superfamily protein
AT3G20993	LCR56	1.55	0.05	low-molecular-weight cysteine-rich 56
AT2G02930	GSTF3	1.55	0.04	glutathione S-transferase F3
AT2G19980	---	1.55	0.00	CAP (Cysteine-rich secretory proteins, Antigen 5, and Pathogenesis-related 1 protein) superfamily protein
AT5G41400	---	1.55	0.07	RING/U-box superfamily protein
AT4G17160	RABB1a	1.55	0.08	RAB GTPase homolog B1A
AT5G38500	---	1.54	0.05	Domain of unknown function (DUF313)
AT2G20670	---	1.54	0.04	Protein of unknown function (DUF506)
AT1G60625	RALFL6	1.53	0.05	RALF-like 6
AT4G32480	---	1.53	0.07	Protein of unknown function (DUF506)
AT3G02620	---	1.53	0.00	Plant stearyl-acyl-carrier-protein desaturase family protein
AT5G26640	---	1.53	0.01	---
AT3G07380	DUF23	1.53	0.01	Domain of unknown function (DUF23)
AT1G22690	---	1.53	0.02	Gibberellin-regulated family protein
AT4G00260	MEE45	1.52	0.01	Transcriptional factor B3 family protein
AT5G40120	AGL76	1.52	0.05	AGAMOUS-like 76
AT5G63160	BT1	1.52	0.08	BTB and TAZ domain protein 1
AT1G19390	---	1.52	0.02	Wall-associated kinase family protein
AT2G07440	---	1.52	0.03	two-component responsive regulator-related / response regulator protein-related
AT4G36820	DUF607	1.51	0.08	Protein of unknown function (DUF607)
AT1G20320	---	1.51	0.06	Haloacid dehalogenase-like hydrolase (HAD) superfamily protein
AT5G23970	---	1.51	0.00	HXXXD-type acyl-transferase family protein
AT4G24660	HB22	1.51	0.06	homeobox protein 22
AT4G22600	---	1.51	0.08	---
AT2G26720	---	1.51	0.01	Cupredoxin superfamily protein
AT1G10652	---	1.50	0.06	---
AT3G18120	---	1.50	0.02	F-box associated ubiquitination effector family protein
AT4G16451	---	1.50	0.07	---
AT4G35190	---	1.49	0.08	Putative lysine decarboxylase family protein
AT3G23860	---	1.49	0.08	GTP-binding protein-related
AT5G36080	---	1.49	0.04	---
AT5G09730	BXL3	1.49	0.07	beta-xylosidase 3
AT4G01470	---	1.49	0.03	tonoplast intrinsic protein 1;3
AT1G07460	---	1.49	0.02	Concanavalin A-like lectin family protein
AT1G62181	---	1.48	0.02	---
AT3G09450	---	1.48	0.05	---
AT1G80660	HA9	1.48	0.08	H(+)-ATPase 9
AT3G43500	---	1.48	0.02	---
AT3G05780	LON3	1.48	0.08	lon protease 3
AT1G72060	---	1.48	0.06	serine-type endopeptidase inhibitors
AT5G56490	---	1.48	0.06	D-arabinono-1,4-lactone oxidase family protein
AT5G39920	---	1.48	0.03	---

Table 8. *CLE2* down-regulated top 100 genes in roots

AGI code	Gene	Fold change	P-value	Description
AT2G19500	CKX2	0.34	0.01	cytokinin oxidase 2
AT1G02920	GSTF7	0.48	0.05	glutathione S-transferase 7
AT2G43000	NAC042	0.50	0.00	NAC domain containing protein 42
AT4G12545	---	0.50	0.01	Bifunctional inhibitor/lipid-transfer protein/seed storage 2S albumin superfamily protein
AT5G56080	NAS2	0.50	0.00	nicotianamine synthase 2
AT2G30750	CYP71A12	0.51	0.07	cytochrome P450, family 71, subfamily A, polypeptide 12
AT1G18970	GLP4	0.51	0.01	germin-like protein 4
AT1G14550	---	0.51	0.01	Peroxidase superfamily protein
AT5G47990	CYP705A5	0.53	0.01	cytochrome P450, family 705, subfamily A, polypeptide 5
AT3G59340	DUF914	0.54	0.00	Eukaryotic protein of unknown function (DUF914)
AT5G64120	---	0.54	0.01	Peroxidase superfamily protein
AT1G52940	PAP5	0.55	0.07	purple acid phosphatase 5
AT2G26560	PLA2A	0.55	0.00	phospholipase A 2A
AT1G74890	ARR15	0.55	0.07	response regulator 15
AT1G09350	GolS3	0.55	0.03	galactinol synthase 3
AT1G23160	---	0.56	0.01	Auxin-responsive GH3 family protein
AT1G30140	---	0.57	0.01	---
AT4G12490	---	0.57	0.00	Bifunctional inhibitor/lipid-transfer protein/seed storage 2S albumin superfamily protein
AT2G20520	FLA6	0.57	0.05	FASCICLIN-like arabinogalactan 6
AT1G14960	---	0.57	0.02	Polyketide cyclase/dehydrase and lipid transport superfamily protein
AT5G24140	SQP2	0.57	0.01	squalene monooxygenase 2
AT5G57220	CYP81F2	0.58	0.01	cytochrome P450, family 81, subfamily F, polypeptide 2
AT5G36140	CYP716A2	0.58	0.08	cytochrome P450, family 716, subfamily A, polypeptide 2
AT1G50930	---	0.58	0.03	---
AT5G39580	---	0.58	0.05	Peroxidase superfamily protein
AT5G48010	THAS1	0.58	0.00	thalianol synthase 1
AT5G65980	---	0.58	0.01	Auxin efflux carrier family protein
AT5G42040	RPN12b	0.58	0.01	regulatory particle non-ATPase 12B
AT4G03039	---	0.58	0.04	MIR826a; miRNA
AT1G14540	---	0.58	0.02	Peroxidase superfamily protein
AT2G15220	---	0.59	0.01	Plant basic secretory protein (BSP) family protein
AT1G31173	---	0.59	0.05	MIR167D; miRNA
AT2G18720	---	0.59	0.03	Translation elongation factor EF1A/initiation factor IF2gamma family protein
AT1G21120	---	0.59	0.06	O-methyltransferase family protein
AT1G67980	CCOAMT	0.59	0.04	caffeoyl-CoA 3-O-methyltransferase
AT5G12340	---	0.59	0.01	---
AT3G53600	---	0.60	0.07	C2H2-type zinc finger family protein
AT1G56410	ERD2	0.60	0.04	heat shock protein 70 (Hsp 70) family protein
AT3G48720	---	0.60	0.02	HXXXD-type acyl-transferase family protein
AT5G64540	---	0.60	0.04	---
AT2G23830	---	0.60	0.02	PapD-like superfamily protein
AT1G10550	XTH33	0.60	0.01	xyloglucan:xyloglucosyl transferase 33
AT5G66690	---	0.60	0.01	UDP-Glycosyltransferase superfamily protein
AT2G40330	PYL6	0.60	0.02	PYR1-like 6
AT1G54970	PRP1	0.60	0.06	proline-rich protein 1
AT1G01183	---	0.60	0.08	MIR165/MIR165A; miRNA
AT1G27550	---	0.61	0.01	F-box family protein
AT5G17050	UGT78D2	0.61	0.03	UDP-glucosyl transferase 78D2
AT2G16505	---	0.61	0.02	Maternally expressed gene (MEG) family protein
AT3G03776	---	0.61	0.05	hydroxyproline-rich glycoprotein family protein

Table 8. (Continued.)

AGI code	Gene	Fold change	P-value	Description
AT2G25160	CYP82F1	0.61	0.02	cytochrome P450, family 82, subfamily F, polypeptide 1
AT4G13450	---	0.61	0.02	Adenine nucleotide alpha hydrolases-like superfamily protein
AT4G12500	---	0.62	0.02	Bifunctional inhibitor/lipid-transfer protein/seed storage 2S albumin superfamily protein
AT1G55591	---	0.62	0.04	MIR158b; miRNA
AT3G01970	WRKY45	0.62	0.01	WRKY DNA-binding protein 45
AT3G63380	---	0.62	0.06	ATPase E1-E2 type family protein / haloacid dehalogenase-like hydrolase family protein
AT1G52857	---	0.62	0.01	---
AT1G77160	---	0.63	0.07	Protein of unknown function (DUF506)
AT5G64110	---	0.63	0.02	Peroxidase superfamily protein
AT1G73120	---	0.63	0.02	---
AT2G40670	RR16	0.63	0.06	response regulator 16
AT4G10310	HKT1	0.63	0.03	high-affinity K ⁺ transporter 1
AT4G29740	CKX4	0.63	0.01	cytokinin oxidase 4
AT3G01760	---	0.63	0.07	Transmembrane amino acid transporter family protein
AT3G29250	---	0.63	0.00	NAD(P)-binding Rossmann-fold superfamily protein
AT2G26370	---	0.63	0.00	MD-2-related lipid recognition domain-containing protein
AT2G23620	MES1	0.63	0.00	methyl esterase 1
AT2G13900	---	0.64	0.01	Cysteine/Histidine-rich C1 domain family protein
AT2G29410	MTPB1	0.64	0.00	metal tolerance protein B1
AT4G15417	RTL1	0.64	0.02	RNAse II-like 1
AT3G52740	---	0.64	0.02	---
AT4G04450	---	0.64	0.05	WRKY family transcription factor
AT2G46790	PRR9	0.64	0.04	pseudo-response regulator 9
AT1G02930	GSTF6	0.64	0.00	glutathione S-transferase 6
AT4G37235	UPF0497	0.64	0.04	Uncharacterised protein family (UPF0497)
AT3G60270	---	0.65	0.04	Cupredoxin superfamily protein
AT1G32385	---	0.65	0.08	snoRNA
AT5G16980	---	0.65	0.01	Zinc-binding dehydrogenase family protein
AT4G00975	---	0.65	0.04	other RNA
AT4G22610	---	0.65	0.07	Bifunctional inhibitor/lipid-transfer protein/seed storage 2S albumin superfamily protein
AT4G39404	---	0.65	0.01	other RNA
AT2G28860	CYP710A4	0.65	0.01	cytochrome P450, family 710, subfamily A, polypeptide 4
AT5G48595	---	0.65	0.06	Defensin-like (DEFL) family protein
AT3G04210	TIR-NBS class	0.65	0.08	Disease resistance protein (TIR-NBS class)
AT1G02360	---	0.66	0.01	Chitinase family protein
AT4G32580	---	0.66	0.02	Thioredoxin superfamily protein
AT5G47980	---	0.66	0.08	HXXXD-type acyl-transferase family protein
AT3G17180	scpl33	0.66	0.04	serine carboxypeptidase-like 33
AT1G66800	---	0.66	0.01	NAD(P)-binding Rossmann-fold superfamily protein
AT2G47460	MYB12	0.66	0.03	myb domain protein 12
AT5G36130	---	0.66	0.07	Cytochrome P450 superfamily protein
AT3G13610	---	0.66	0.05	2-oxoglutarate (2OG) and Fe(II)-dependent oxygenase superfamily protein
AT5G53990	---	0.66	0.06	UDP-Glycosyltransferase superfamily protein
AT5G38100	---	0.66	0.06	S-adenosyl-L-methionine-dependent methyltransferases superfamily protein
AT1G68640	PAN	0.66	0.02	bZIP transcription factor family protein
AT1G64405	---	0.66	0.05	---
AT1G28230	PUP1	0.66	0.03	purine permease 1
AT4G17670	DUF581	0.66	0.02	Protein of unknown function (DUF581)
AT4G12170	---	0.66	0.05	Thioredoxin superfamily protein
AT5G38710	---	0.67	0.00	Methylenetetrahydrofolate reductase family protein

At1g73165 (CLE1) **RLSPGGPDPRHH**
At4g18510 (CLE2) **RLSPGGPDQHH**
At1g06225 (CLE3) **RLSPGGPDPRHH**
At2g31081 (CLE4) **RLSPGGPDPRHH**
At2g31083 (CLE5) **RVSPGGPDQHH**
At2g31085 (CLE6) **RVSPGGPDQHH**
At2g31082 (CLE7) **RFSPGGPDQHH**

Fig. 1 Amino acid sequence alignments of the CLE domains of CLE1–7 peptides.

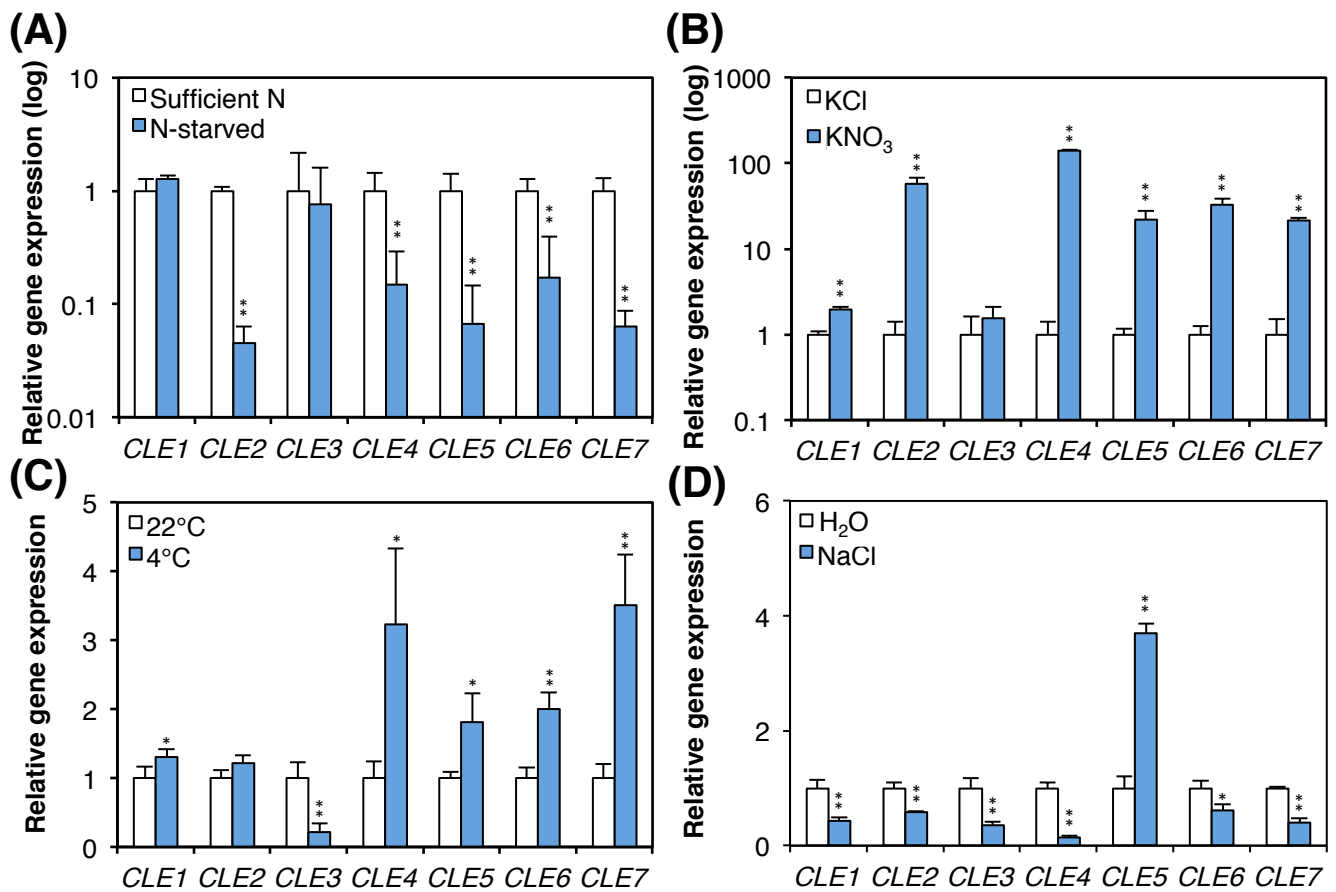


Fig. 2 Quantitative real-time PCR (qRT-PCR) analysis of *CLE1*–*CLE7* in *Arabidopsis* under different abiotic stresses. **A–D** Expression analysis of *CLE* genes in whole seedlings (**A–C**) or roots (**D**) upon nitrate starvation (**A**), nitrate replenishment (**B**), cold treatment (**C**) and salt treatment (**D**). In (**A**), 5-day-old WT seedlings grown in full nutrition liquid medium were further cultured with (sufficient N) or without nitrogen (N-starved) for 3 days. In (**B**), N-starved seedlings used in (**A**) were incubated in the presence of 3 mM KNO_3 or KCl (control) for 3 h. In (**C**), 10-day-old seedlings grown on a conventional solid medium were incubated at 4°C for 12 h. In (**D**), 10-day-old seedlings grown on a conventional solid medium were further cultured with or without 150 mM NaCl for 24 h. Data represent mean \pm standard deviation (SD) of three replicates. Asterisks indicate significant differences (* $P < 0.05$, ** $P < 0.01$; Welch's t-test).

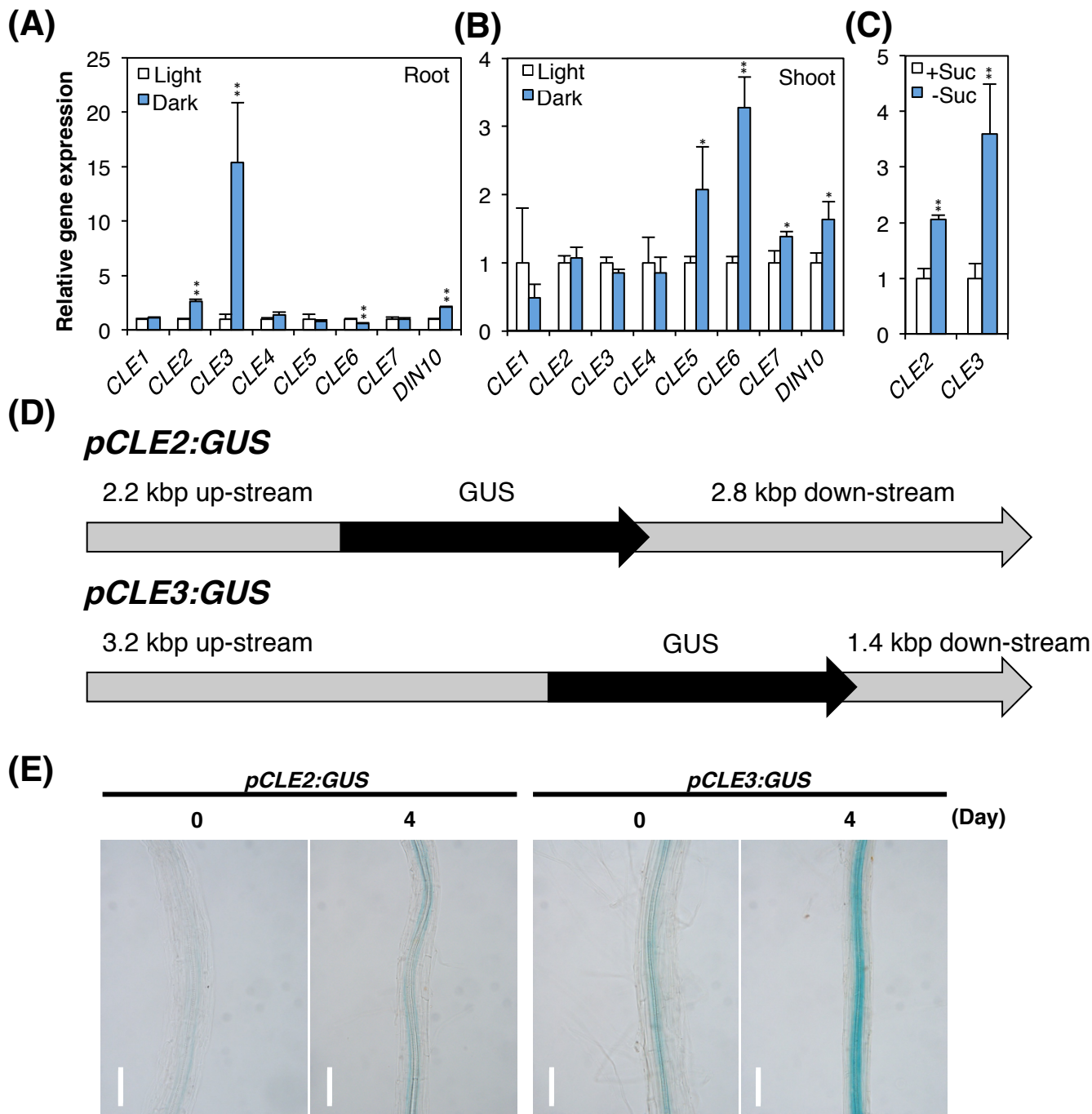


Fig. 3 *CLE2* and *CLE3* expression upon dark treatment. Transcript levels were measured by qRT-PCR (**A–C**) and transcriptional activities were visualized by GUS reporter constructs (**E**). Transcriptional responses of *CLE1* to *CLE7* in roots (**A**) and shoots (**B**) upon dark treatment. Nine-day-old wild-type seedlings grown on a conventional solid medium were further cultured in dark for 48 h. *DIN10* was used as positive control. **C** Transcriptional responses of *CLE2* and *CLE3* upon sucrose starvation. Nine-day-old seedlings were transferred to a solid media deprived of sucrose and incubated for 48 h. Data represent mean \pm SD of three replicates. Asterisks indicate significant differences (* $P < 0.05$, ** $P < 0.01$; Welch's t-test). **D** Preparation of *CLE2* and *CLE3* GUS reporters. Both up- and down-stream sequences were amplified as illustrates above. Primers used in this process were listed up in Table 13. **E** *CLE2* and *CLE3* promoter activities. Plants harboring the promoter-GUS reporter constructs were incubated on a solid medium for 9 days, further grown on a soil for 2 weeks, and sampled before and after 4 days of darkness. Scale bars indicate 100 μ m.

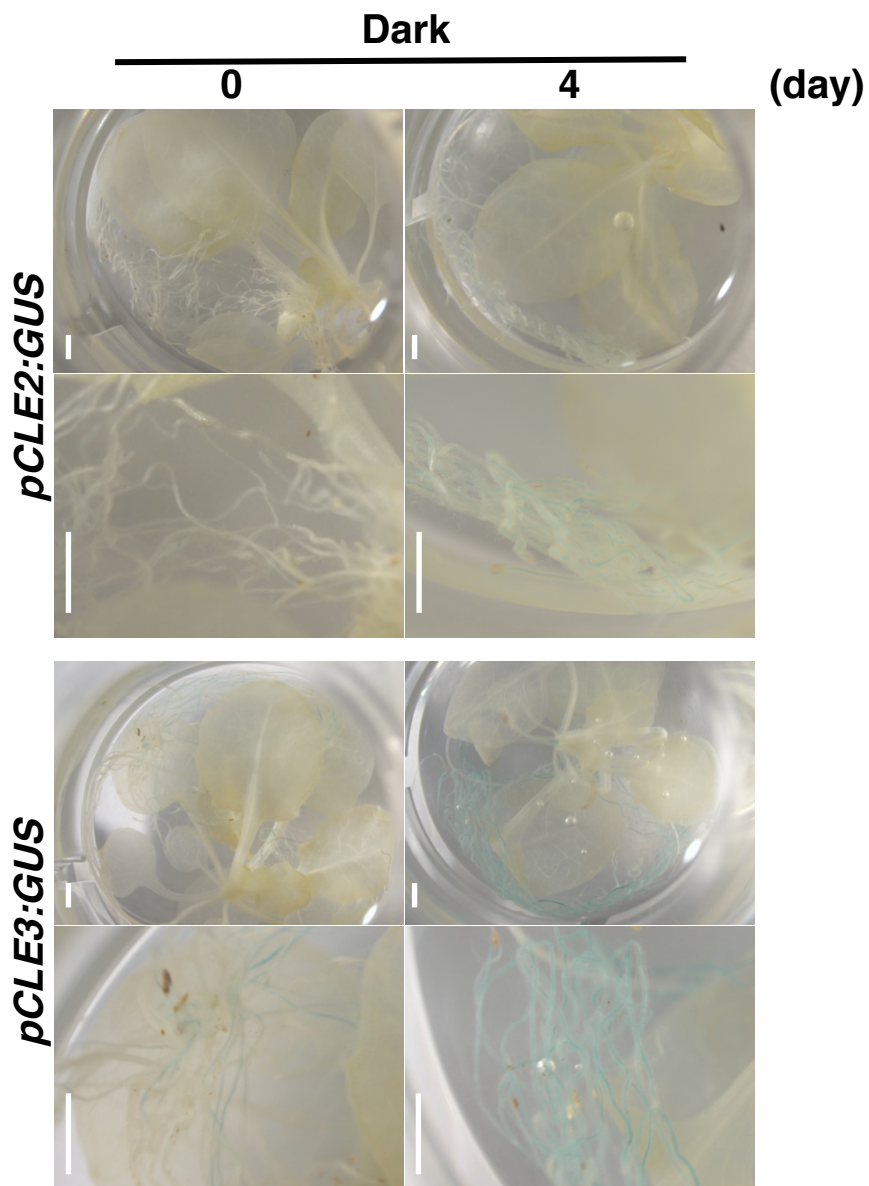


Fig. 4 *CLE2* and *CLE3* promoter activities determined by GUS reporter assays. Plants harboring the promoter-GUS reporter constructs were incubated on a solid medium for 9 days. Then, the plants were grown on soil for 2 weeks and sampled before and after 4 days of dark treatment. Scale bars: 1 mm.

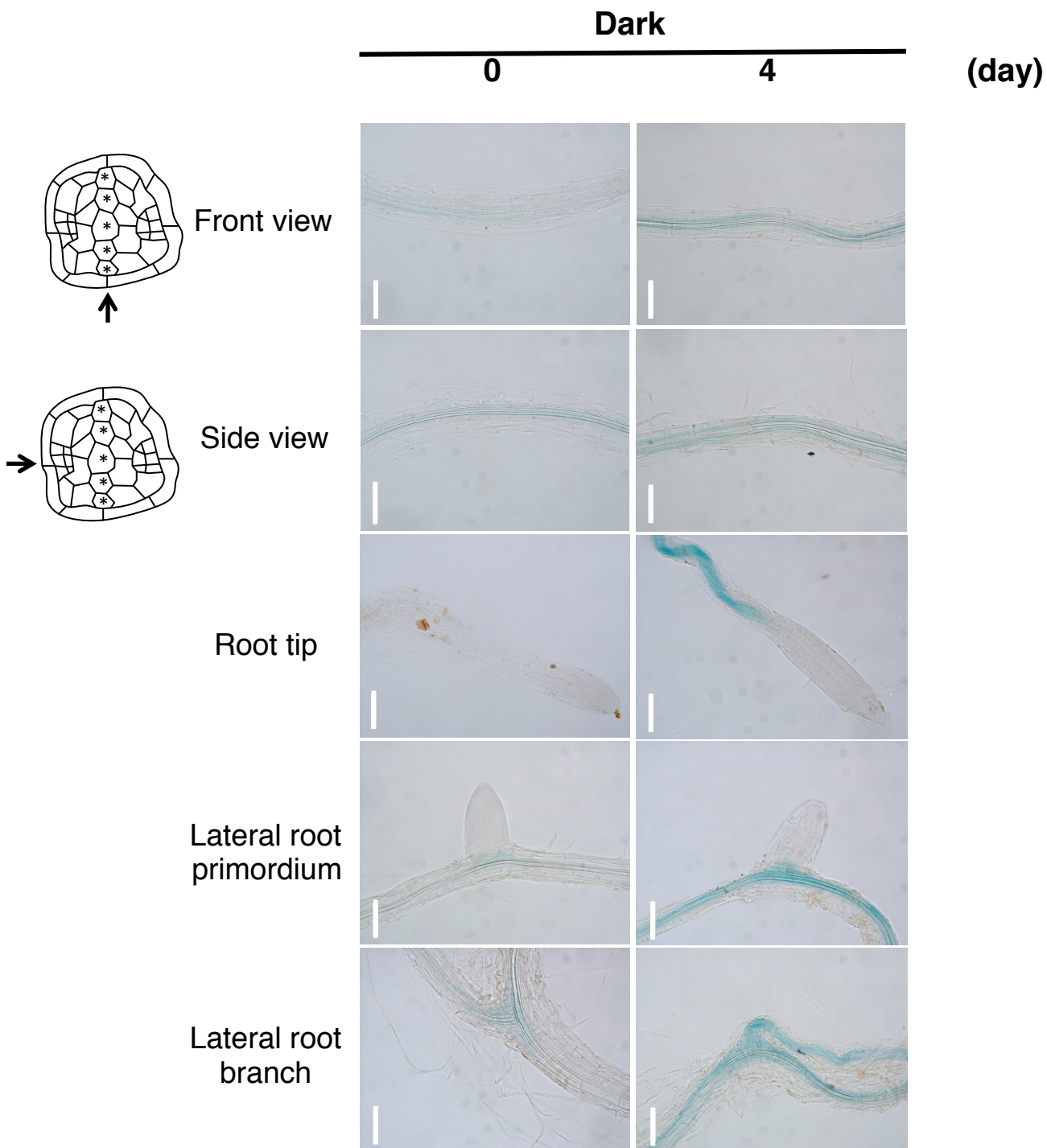


Fig. 5 Close-up of *CLE2* promoter activities in roots determined by GUS reporter assays. Plants harboring the promoter-GUS reporter constructs were incubated on a solid medium for 9 days. Then, the plants were grown on soil for 2 weeks and sampled before and after 4 days of dark treatment. The front view was showed in Fig. 3E. Arrows beside the schematic diagram indicate the angle of view. Asterisks indicate xylem cells. Scale bars: 100 μ m.

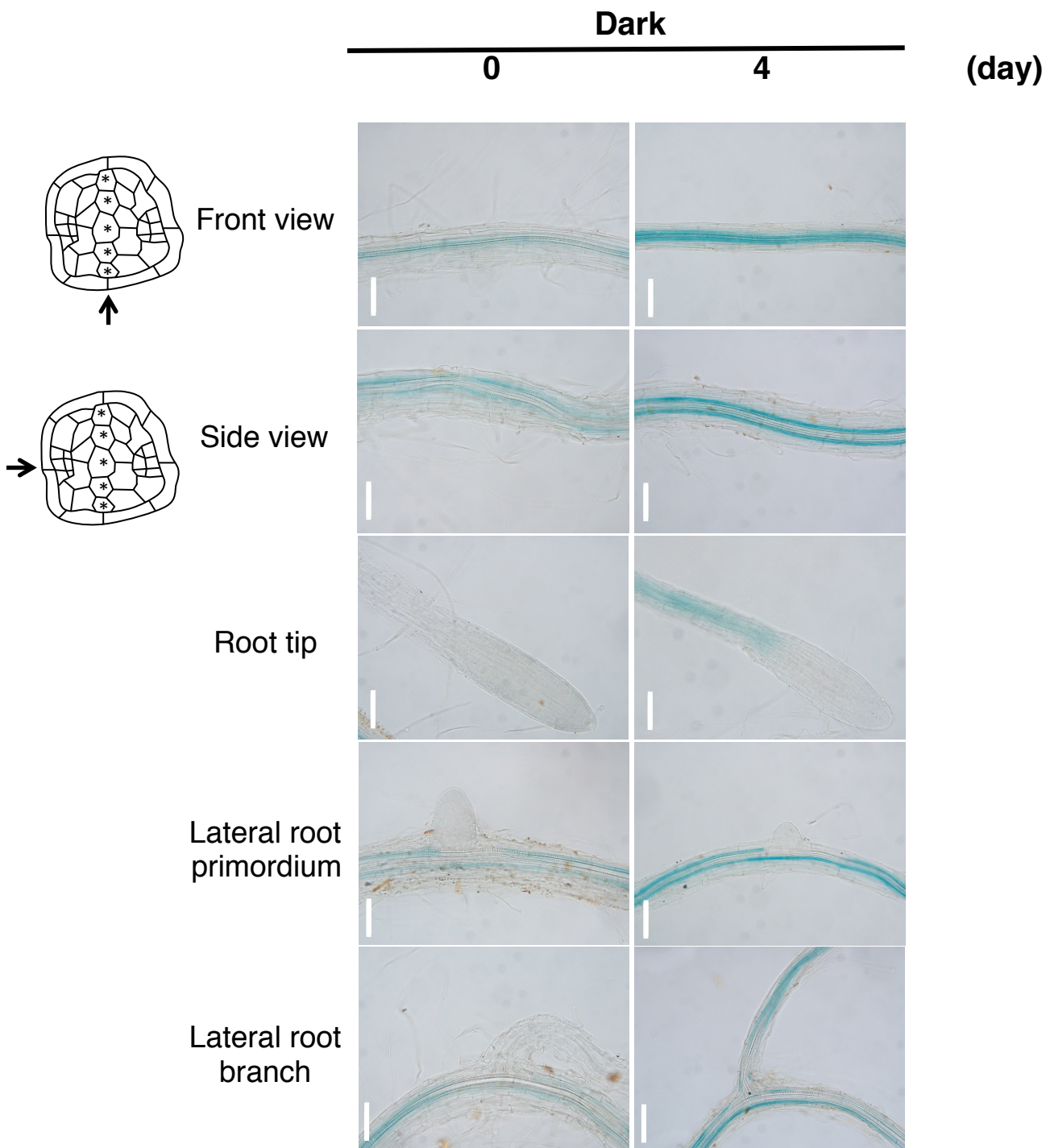
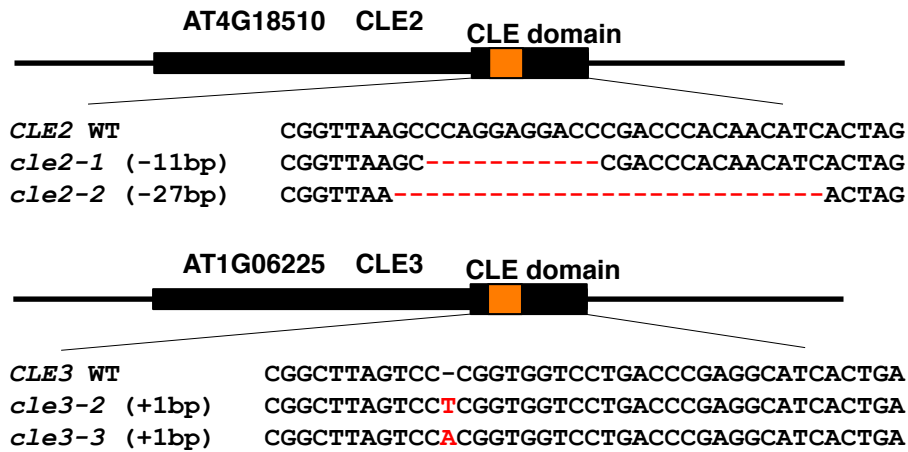


Fig. 6 Close-up of *CLE3* promoter activities in roots determined by GUS reporter assays. Plants harboring the promoter-GUS reporter constructs were incubated on a solid medium for 9 days. Then, the plants were grown on soil for 2 weeks and sampled before and after 4 days of dark treatment. The front view was showed in Fig. 3E. Arrows beside the schematic diagram indicate the angle of view. Asterisks indicate xylem cells. Scale bars: 100 μ m.

(A)



(B)

CLE2 WT RLSPGGPDPQHH*
cle2-1 RLS^{RPTTSLVILCFSISSTCLLLINNLVATKLEFFFFVINLRIYVCHNTTKLVTVL}*
cle2-2 RL^N*

CLE3 WT RLSPGGPDPRHH*
cle3-2 RLSP^{RWS}*
Cle3-3 RLSP^{RWS}*

Fig. 7 *cle2* and *cle3* mutants generated using the CRISPR/Cas9 system. **A** Insertions and deletions in the CLE domains of *cle2* and *cle3*. **B** Amino acid sequences of the CLE domains of *cle2* and *cle3* mutant variants. Asterisks represent stop codons.

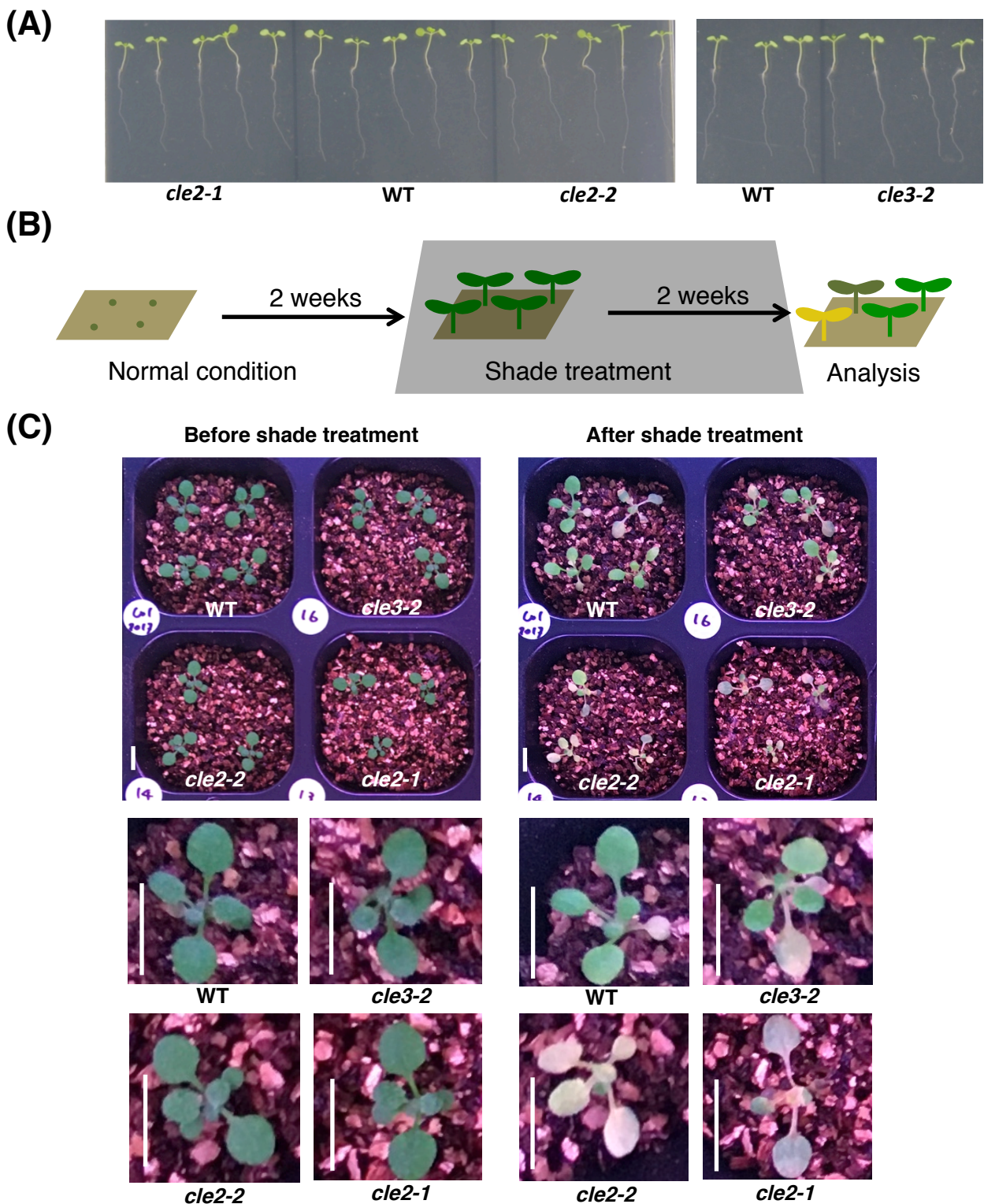


Fig. 8 Phenotypic characterization of *cle2* mutant plants grown under the shade treatment. **A** *cle2* and *cle3* did not show any growth defects under normal growth conditions. **B** Flow chart showing the shade treatment. WT, *cle2-1*, *cle2-2* and *cle3-2* plants were grown under long days for 2 weeks and then subjected to insufficient light for another 2 weeks. **C** Growth defect of *cle2* plants subjected to the shade treatment. Close-up of seedling of each genotype was shown. Scale bars: 5 mm.

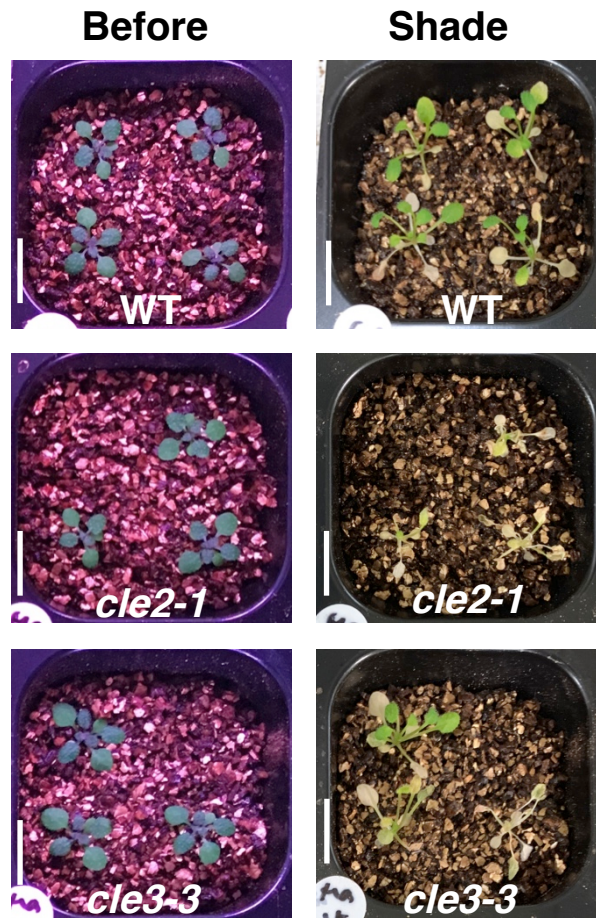
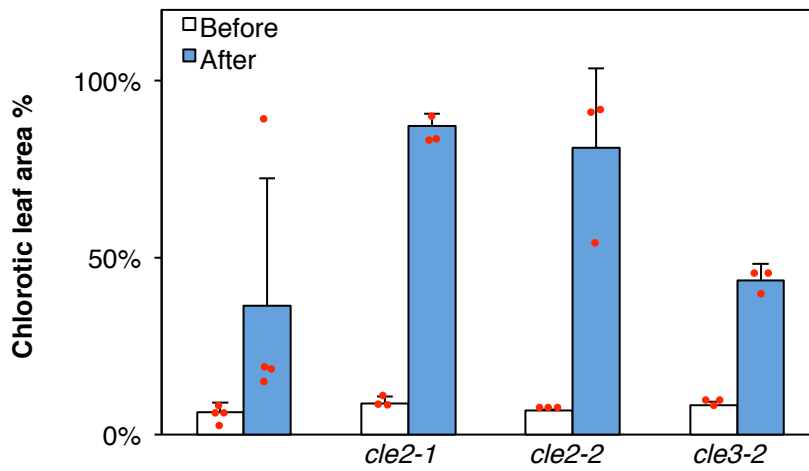


Fig. 9 Experimental replicates of *cle2* and *cle3* mutants under the shade treatment. Scale bars: 10 mm.

(A)



(B)

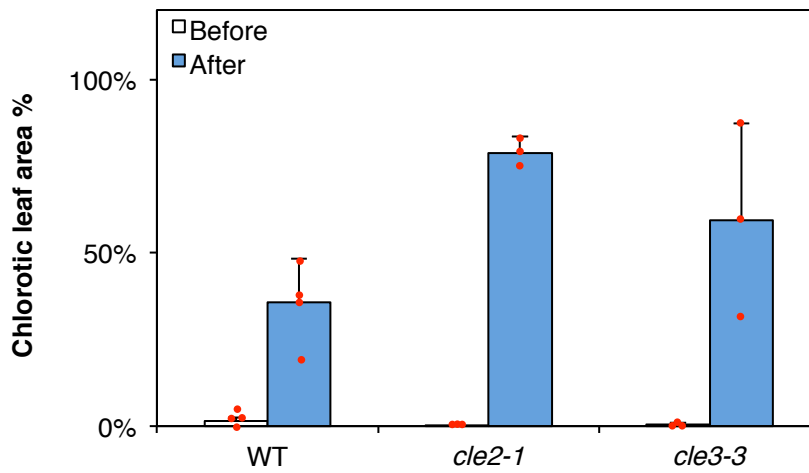


Fig. 10 Quantification of chlorotic leaf area of plants shown in Fig. 8C (A) and Fig. 9 (B). Data represent mean \pm SD of three (*cle* lines) or four (WT) replicates. Red spots indicate the percentage of chlorotic leaf area of each seedling.

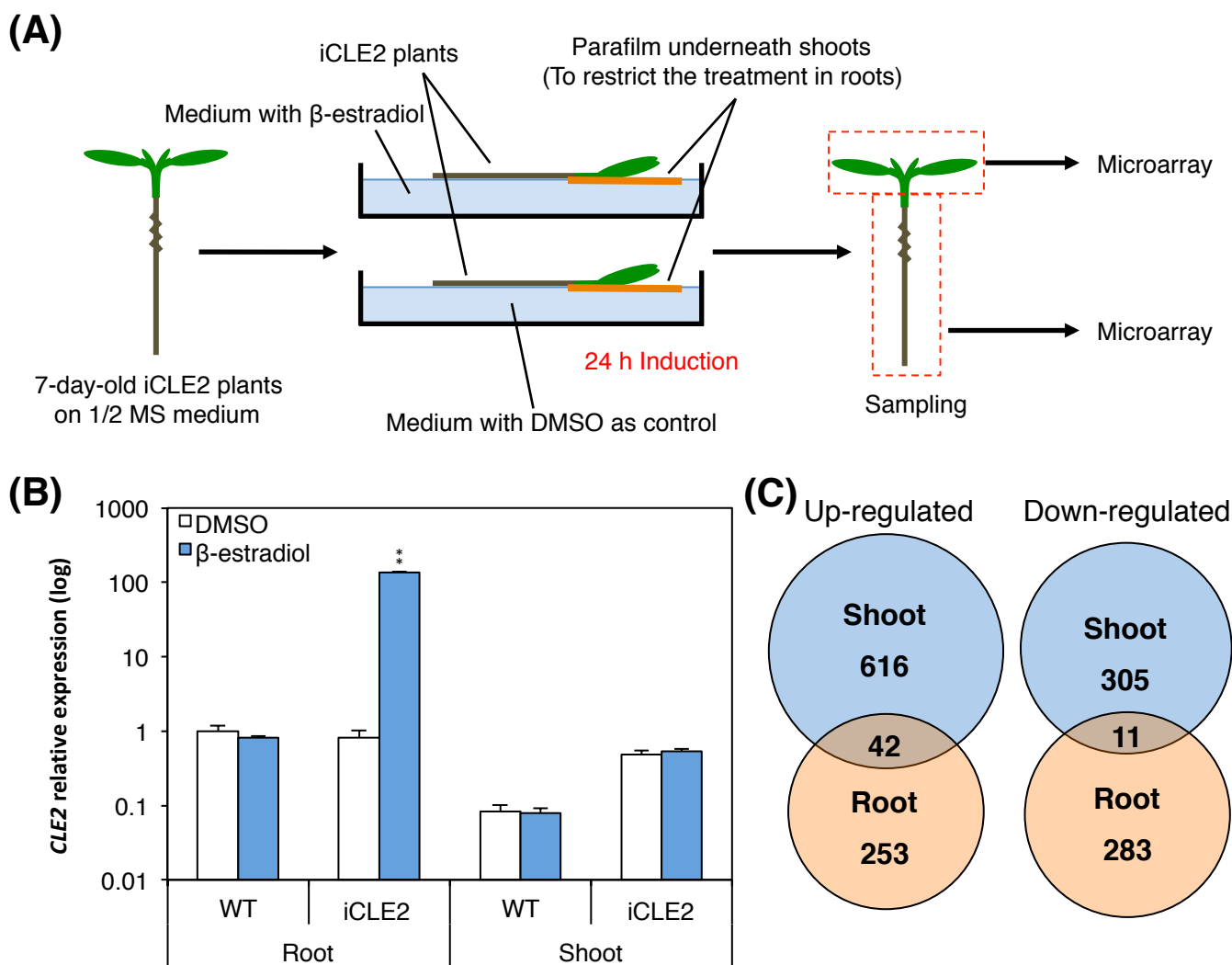


Fig. 11 Transcriptome analysis of transgenic iCLE2 Arabidopsis plants expressing *CLE2* under the control of the estradiol-inducible promoter. **A** Flow chart showing the induction of *CLE2* expression in iCLE2 plants. Roots of 7-day-old iCLE2 plants were treated with 5 mM β -estradiol for 24 h. After the 24-h induction, roots and shoots of iCLE2 plants were sampled separately and used for microarray analysis. DMSO-treated iCLE2 plants served as a control. Three biological replicates were performed. **B** *CLE2* transcript levels in WT and iCLE2 plants treated with β -estradiol or DMSO. Data represent mean \pm SD of three biological replicates. Asterisks indicate significant differences (** $P < 0.01$; Welch's t-test). **C** Number of genes up- or down-regulated (fold-change > 1.35 or $< 1.35^{-1}$, respectively) in roots and shoots of β -estradiol-induced iCLE2 plants. Genes with significant differences in expression level are shown ($P < 0.1$; Student's t-test).

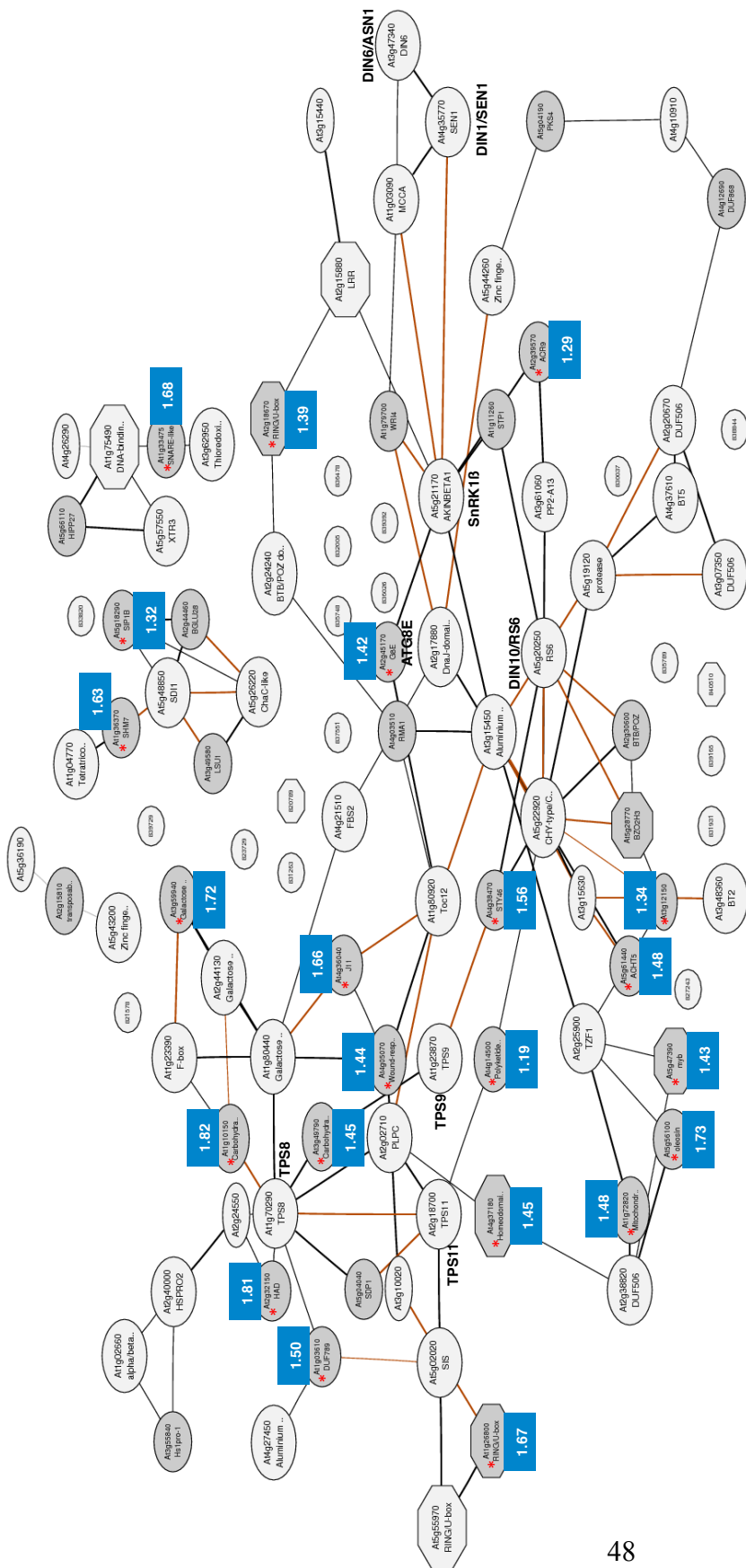


Fig. 12 Coexpression network of top 100 genes up-regulated in the shoots of iCLE2 plants upon the induction of *CLE2*. The coexpression network was drawn using ATTED-II ver.9.2 (<http://atted.jp>). Lines of different width and color indicate a range of gene coexpression levels in ATTED-II. Octagonal nodes indicate transcriptional factors. Light gray nodes indicate top 100 genes regulated by *CLE2*. Dark gray nodes indicate genes correlated with at least 2 of the top 100 genes. Nodes with asterisks and numbers indicate genes regulated by *CLE2* with indicated fold-changes in shoots (Table 7).

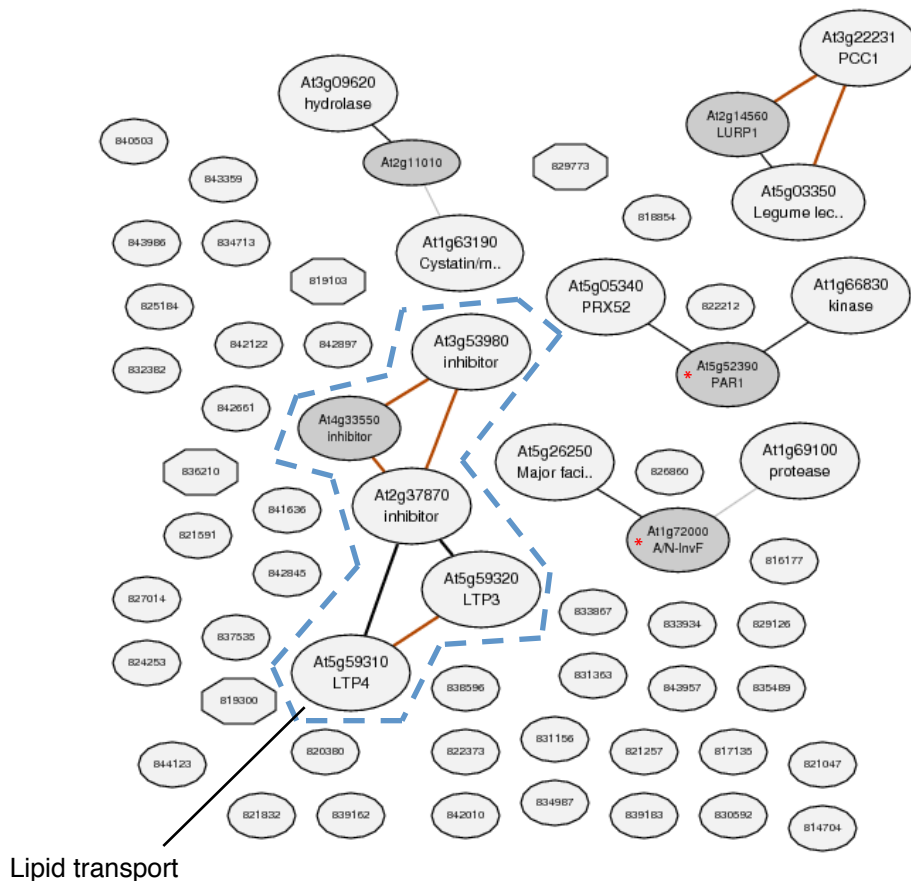


Fig. 13 Coexpression network of top 100 genes down-regulated in the shoots of iCLE2 plants upon the induction of *CLE2*. Coexpression network was drawn using ATTED-II ver.9.2 (<http://atted.jp>). Lines of different width and color indicate a range of gene coexpression levels in ATTED-II. Light gray nodes indicate top 100 genes that shared similar coexpression networks. Dark gray nodes indicate genes coexpressed with at least 2 of the top 100 genes. Nodes with asterisks indicate *CLE2*-regulated genes in shoots that not included in the top 100 genes (Table 8).

References

- Alford, S. R., Rangarajan, P., Williams, S. P. and Gillasp, G. E. (2012).** myo-Inositol oxygenase is required for responses to low energy conditions in *Arabidopsis thaliana*. *Front. Plant Sci.* **3**, 69.
- Aoki, Y., Okamura, Y., Tadaka, S., Kinoshita, K. and Obayashi, T. (2016).** ATTED-II in 2016: a plant coexpression database towards lineage-specific coexpression. *Plant Cell Physiol.* **57**, e5.
- Araya, T., Miyamoto, M., Wibowo, J., Suzuki, A., Kojima, S., Tsuchiya, Y. N., Sawa, S., Fukuda, H., Wirén, N. V. and Takahashi, H. (2014).** CLE-CLAVATA1 peptide-receptor signaling module regulates the expansion of plant root systems in a nitrogen-dependent manner. *Proc. Natl. Acad. Sci. U.S.A.* **111**, 2029-2034.
- Baena-González, E. and Sheen, J. (2008).** Convergent energy and stress signaling. *Trends Plant Sci.* **13**, 474-482.
- Baena-González, E., Rolland, F., Thevelein, J. M. and Sheen, J. (2007).** A central integrator of transcription networks in plant stress and energy signalling. *Nature* **448**, 938-942.
- Bidadi, H., Matsuoka, K., Sage-Ono, K., Fukushima, J., Pitaksaringkarn, W., Asahina, M., Yamaguchi, S., Sawa, S., Fukuda, H., Matsubayashi, Y., Ono, M. and Satoh, S. (2014).** *CLE6* expression recovers gibberellin deficiency to promote shoot growth in *Arabidopsis*. *Plant J.* **78**, 241-252.
- Bonetta, D. and McCourt, P. (1998)** Genetic analysis of ABA signal transduction pathways. *Trends Plant Sci.* **3**, 231-235.
- Brand, U., Fletcher, J. C., Hobe, M., Meyerowitz, E. M. and Simon, R. (2000).** Dependence of stem cell fate in *Arabidopsis* on a feedback loop regulated by CLV3

activity. *Science* **289**, 617-619.

Bray, E.A. (1997) Plant responses to water deficit. *Trends Plant Sci.* **2**: 48–53. **Choi, H., Hong, J., Ha, J., Kang, J. and Kim, S.Y.** (2000) ABFs, a family of ABA-responsive element binding factors. *J. Biol. Chem.* **275**, 1723-1730.

Clark, S. E., Jacobsen, S. E., Levin, J. Z. and Meyerowitz, E. M. (1996). The CLAVATA and SHOOT MERISTEMLESS loci competitively regulate meristem activity in *Arabidopsis*. *Development* **122**, 1567-1575.

Curtis, M. D. and Grossniklaus, U. (2003). A gateway cloning vector set for high-throughput functional analysis of genes in planta. *Plant Physiol.* **133**, 462- 469.

DiGennaro, P., Grienberger, E., Dao, T. Q., Jun, J. H. and Fletcher, J. C. (2018). Peptide signaling molecules CLE5 and CLE6 affect *Arabidopsis* leaf shape downstream of leaf patterning transcription factors and auxin. *Plant Direct* **2**, e00103.

Endo, S., Iwai, Y., and Fukuda, H. (2019). Cargo-dependent and cell wall-associated xylem transport in *Arabidopsis*. *New Phytol.* **222**, 159-170.

Endo, S., Iwamoto, K. and Fukuda, H. (2018). Overexpression and cosuppression of xylem-related genes in an early xylem differentiation stage-specific manner by the AtTED4 promoter. *Plant Biotechnol. J.* **16**, 451-458.

Endo, S., Shinohara, H., Matsubayashi, Y. and Fukuda, H. (2013). A novel pollen-pistil interaction conferring high-temperature tolerance during reproduction via CLE45 signaling. *Curr. Biol.* **23**, 1670-1676.

Finkelstein, R.R., Gampala, S.S.L. and Rock, C.D. (2002) Absciscic acid signaling in seeds and seedlings. *Plant Cell* **14**, S15-S45.

Fujiki, Y., Yoshikawa, Y., Sato, T., Inada, N., Ito, M., Nishida, I. and Watanabe, A. (2001). Dark-inducible genes from *Arabidopsis thaliana* are associated with leaf senescence and repressed by sugars. *Physiol. Plant.* **111**, 345-352.

Han, H., Liu, X., and Zhou, Y. (2020). Transcriptional circuits in control of shoot stem cell homeostasis. *Curr. Opin. Plant Biol.* **53**, 50-56.

Hirakawa, Y., Kondo, Y. and Fukuda, H. (2010). TDIF peptide signaling regulates vascular stem cell proliferation via the WOX4 homeobox gene in Arabidopsis. *Plant Cell* **22**, 2618-2629.

Hirakawa, Y., Shinohara, H., Kondo, Y., Inoue, A., Nakanomyo, I., Ogawa, M., Sawa, S., Ohashi-Ito, K., Matsubayashi, Y. and Fukuda, H. (2008). Non-cell-autonomous control of vascular stem cell fate by a CLE peptide/receptor system. *Proc. Natl. Acad. Sci. U.S.A.* **105**, 15208-15213.

Hobe, M., Müller, R., Grünwald, M., Brand, U. and Simon, R. (2003). Loss of CLE40, a protein functionally equivalent to the stem cell restricting signal CLV3, enhances root waving in Arabidopsis. *Dev. Genes Evol.* **213**, 371-381.

Huang, D. W., Sherman, B. T., Zheng, X., Yang, J., Imamichi, T., Stephens, R. and Lempicki, R. A. (2009). Extracting biological meaning from large gene lists with DAVID. *Curr. Protoc. Bioinformatics* **27**, 13-11.

Ito, Y., Nakanomyo, I., Motose, H., Iwamoto, K., Sawa, S., Dohmae, N. and Fukuda, H. (2006). Dodeca-CLE peptides as suppressors of plant stem cell differentiation. *Science* **313**, 842-845.

Jossier, M., Bouly, J. P., Meimoun, P., Arjmand, A., Lessard, P., Hawley, S., Haridie, D. G. and Thomas, M. (2009). SnRK1 (SNF1-related kinase 1) has a central role in sugar and ABA signalling in *Arabidopsis thaliana*. *Plant J.* **59**, 316-328.

Jun, J., Fiume, E., Roeder, A. H., Meng, L., Sharma, V. K., Osmont, K. S., Baker, C., Ha, C. M., Meyerowitz, E. M., Feldman, L. J. and Fletcher, J. C. (2010). Comprehensive analysis of *CLE* polypeptide signaling gene expression and

overexpression activity in Arabidopsis. *Plant Physiol.* **154**, 1721-1736.

Kayes, J. M. and Clark, S. E. (1998). CLAVATA2, a regulator of meristem and organ development in Arabidopsis. *Development* **125**, 3843-3851.

Kinoshita, A., Nakamura, Y., Sasaki, E., Kyojuka, J., Fukuda, H., and Sawa, S. (2007). Gain-of-function phenotypes of chemically synthetic CLAVATA3/ESR-related (CLE) peptides in *Arabidopsis thaliana* and *Oryza sativa*. *Plant Cell Physiol.* **48**, 1821-1825.

Kondo, Y., Hirakawa, Y., Kieber, J. J. and Fukuda, H. (2011). CLE peptides can negatively regulate protoxylem vessel formation via cytokinin signaling. *Plant Cell Physiol.* **52**, 37-48.

Kucukoglu, M., and Nilsson, O. (2015). CLE peptide signaling in plants—the power of moving around. *Physiol. Plant.* **155**, 74-87.

Matsubayashi, Y. (2011). Small post-translationally modified peptide signals in Arabidopsis. *Arabidopsis Book* **9**, e0150.

Matsubayashi, Y. and Sakagami, Y. (1996). Phytosulfokine, sulfated peptides that induce the proliferation of single mesophyll cells of *Asparagus officinalis* L. *Proc. Natl. Acad. Sci. U.S.A.* **93**, 7623-7627.

Mayer, K. F., Schoof, H., Haecker, A., Lenhard, M., Jürgens, G. and Laux, T. (1998). Role of WUSCHEL in regulating stem cell fate in the Arabidopsis shoot meristem. *Cell* **95**, 805-815.

McDowell, N., Pockman, W. T., Allen, C. D., Breshears, D. D., Cobb, N., Kolb, T., Plaut, J., Sperry, J., West, A., Williams, D. G. and Yezpez, E. A. (2008). Mechanisms of plant survival and mortality during drought: why do some plants survive while others succumb to drought? *New Phytol.* **178**, 719–739.

- Morita, J., Kato, K., Nakane, T., Kondo, Y., Fukuda, H., Nishimasu, H., Ishitani, R. and Nureki, O.** (2016). Crystal structure of the plant receptor-like kinase TDR in complex with the TDIF peptide. *Nat. Commun.* **7**, 12383.
- Mosher, S., Seybold, H., Rodriguez, P., Stahl, M., Davies, K. A., Dayaratne, S., Morillo, S. A., Wierzbica, M., Favery, B., Keller, H., Tax, F. E. and Kemmerling, B.** (2013). The tyrosine-sulfated peptide receptors PSKR1 and PSY1R modify the immunity of *Arabidopsis* to biotrophic and necrotrophic pathogens in an antagonistic manner. *Plant J.* **73**, 469-482.
- Ni, J. and Clark, S. E.** (2006). Evidence for functional conservation, sufficiency, and proteolytic processing of the CLAVATA3 CLE domain. *Plant Physiol.* **140**, 726-733.
- Obayashi, T., Hayashi, S., Saeki, M., Ohta, H. and Kinoshita, K.** (2009). ATTED-II provides coexpressed gene networks for *Arabidopsis*. *Nucleic Acids Res.* **37**, D987-D991.
- Oelkers, K., Goffard, N., Weiller, G. F., Gresshoff, P. M., Mathesius, U. and Frickey, T.** (2008). Bioinformatic analysis of the CLE signaling peptide family. *BMC Plant Biol.* **8**, 1471-2229.
- Ohashi-Ito, K., Saegusa, M., Iwamoto, K., Oda, Y., Katayama, H., Kojima, M., Sakakibara, H. and Fukuda, H.** (2014). A bHLH complex activates vascular cell division via cytokinin action in root apical meristem. *Curr. Biol.* **24**, 2053-2058.
- Ohyama, K., Shinohara, H., Ogawa-Ohnishi, M. and Matsubayashi, Y.** (2009). A glycopeptide regulating stem cell fate in *Arabidopsis thaliana*. *Nat. Chem. Biol.* **5**, 578-580.
- Okamoto, S., Ohnishi, E., Sato, S., Takahashi, H., Nakazono, M., Tabata, S. and Kawaguchi, M.** (2009). Nod factor/nitrate-induced CLE genes that drive HAR1-mediated systemic regulation of nodulation. *Plant Cell Physiol.* **50**, 67-77.

Plancot, B., Santaella, C., Jaber, R., Kiefer-Meyer, M. C., Follet-Gueye, M. L., Leprince, J., Gattin, I., Souc, C., Driouich, A. and Vitré-Gibouin, M. (2013). Deciphering the responses of root border-like cells of *Arabidopsis* and flax to pathogen-derived elicitors. *Plant physiol.* **163**, 1584-1597.

Polge, C., and Thomas, M. (2007). SNF1/AMPK/SnRK1 kinases, global regulators at the heart of energy control? *Trends Plant Sci.* **12**, 20-28.

Qian, P., Song, W., Yokoo, T., Minobe, A., Wang, G., Ishida, T., Sawa, S., Chai J. and Kakimoto, T. (2018). The CLE9/10 secretory peptide regulates stomatal and vascular development through distinct receptors. *Nat. Plants* **4**, 1071-1081.

Ramon, M., and Rolland, F. (2007). Plant development: introducing trehalose metabolism. *Trends Plant Sci.* **12**, 185-188.

Saito, M., Kondo, Y., and Fukuda, H. (2018). BES1 and BZR1 redundantly promote phloem and xylem differentiation. *Plant Cell Physiol.* **59**, 590-600.

Sato, H., Takasaki, H., Takahashi, F., Suzuki, T., Iuchi, S., Mitsuda, N., Ohme-Takagi, M., Ikeda, M., Seo, M., Yamaguchi-Shinozaki, K., Shinozaki, K. (2018). *Arabidopsis thaliana* NGATHA1 transcription factor induces ABA biosynthesis by activating NCED3 gene during dehydration stress. *Proc. Natl. Acad. Sci. U.S.A.* **115**, E11178-E11187.

Sawa, S., Kinoshita, A., Nakanomyo, I. and Fukuda, H. (2006). CLV3/ESR-related (CLE) peptides as intercellular signaling molecules in plants. *Chemical Rec.* **6**, 303-310.

Scheible, W. R., Morcuende, R., Czechowski, T., Fritz, C., Osuna, D., Palacios-Rojas, N., Schindelasch, D., Thimm, O., Udvardi, M. K. and Stitt, M. (2004). Genome-wide reprogramming of primary and secondary metabolism, protein synthesis, cellular growth processes, and the regulatory infrastructure of *Arabidopsis*

in response to nitrogen. *Plant Physiol.* **136**, 2483-2499.

Schoof, H., Lenhard, M., Haecker, A., Mayer, K. F., Jürgens, G. and Laux, T. (2000). The stem cell population of Arabidopsis shoot meristems is maintained by a regulatory loop between the CLAVATA and WUSCHEL genes. *Cell* **100**, 635- 644.

Shinozaki, K. and Yamaguchi-Shinozaki, K. (1997) Gene expression and signal transduction in water-stress response. *Plant Physiol.* **115**, 327–334.

Stahl, Y., Wink, R. H., Ingram, G. C. and Simon, R. (2009). A signaling module controlling the stem cell niche in Arabidopsis root meristems. *Curr. Biol.* **19**, 909-914.

Strabala, T. J., O'Donnell, P. J., Smit, A. M., Ampomah-Dwamena, C., Martin, E. J., Netzler, N., Nieuwenhuizen, N. J., Quinn, B. D., Foote, H. C. and Hudson, K. R. (2006). Gain-of-function phenotypes of many CLAVATA3/ESR genes, including four new family members, correlate with tandem variations in the conserved CLAVATA3/ESR domain. *Plant Physiol.* **140**, 1331-1344.

Tabata, R., Sumida, K., Yoshii, T., Ohyama, K., Shinohara, H. and Matsubayashi, Y. (2014). Perception of root-derived peptides by shoot LRR-RKs mediates systemic N-demand signaling. *Science* **346**, 343-346.

Takahashi, F., Suzuki, T., Osakabe, Y., Betsuyaku, S., Kondo, Y., Dohmae, N., Fukuda, H., Yamaguchi-Shinozaki, K. and Shinozaki, K. (2018). A small peptide modulates stomatal control via abscisic acid in long-distance signalling. *Nature* **556**, 235-238.

Verma, V., Ravindran, P. and Kumar, P. P. (2016). Plant hormone-mediated regulation of stress responses. *BMC Plant Biol.* **16**, 86.

Vernooij, B., Friedrich, L., Morse, A., Reist, R., Kolditz-Jawhar, R., Ward, E., Uknes, S., Kessmann, H., and Ryals, J. (1994). Salicylic acid is not the translocated signal responsible for inducing systemic acquired resistance but is required in signal

transduction. *Plant Cell* **6**, 959-965.

Xiao, S., Gao, W., Chen, Q. F., Chan, S. W., Zheng, S. X., Ma, J., Wang, M., Welti, R. and Chye, M. L. (2010). Overexpression of Arabidopsis acyl-CoA binding protein ACBP3 promotes starvation-induced and age-dependent leaf senescence. *Plant Cell* **22**, 1463-1482.

Yamaguchi, Y. L., Ishida, T., Yoshimura, M., Imamura, Y., Shimaoka, C., and Sawa, S. (2017). A collection of mutants for CLE-peptide-encoding genes in Arabidopsis generated by CRISPR/Cas9-mediated gene targeting. *Plant Cell Physiol.* **58**, 1848-1856.

Yoro, E., Suzaki, T., and Kawaguchi, M. (2020). CLE-HAR1 systemic signaling and NIN-mediated local signaling suppress the increased rhizobial infection in the daphne mutant of *Lotus japonicus*. *Mol. Plant Microbe Interact.* **33**, 320-327.

Zhang, H., Lin, X., Han, Z., Qu, L. J. and Chai, J. (2016). Crystal structure of PXY-TDIF complex reveals a conserved recognition mechanism among CLE peptide-receptor pairs. *Cell Res.* **26**, 543-555.

Zhang, L., Shi, X., Zhang, Y., Wang, J., Yang, J., Ishida, T., Jiang, W., Han, X., Kang, J., Wang, X., Pan, L., Lv, S., Cao, B., Zhang, Y., Wu, J., Han, H., Hu, Z., Cui, L., Sawa, S., He, J. and Wang, G. (2019). CLE9 peptide-induced stomatal closure is mediated by abscisic acid, hydrogen peroxide, and nitric oxide in *Arabidopsis thaliana*. *Plant Cell Environ.* **42**, 1033-1044.

Zhang, Y., Primavesi, L. F., Jhurrea, D., Andralojc, P. J., Mitchell, R. A. C., Powers, S. J., Schluepmann, H., Delatte, T., Wingler, A. and Paul, M. J. (2009). Inhibition of SNF1-related protein kinase1 activity and regulation of metabolic pathways by trehalose-6-phosphate. *Plant Physiol.* **149**, 1860–1871.